SUPPLEMENTARY MATERIAL

Optimization of Extraction for Diterpenoids from *Euphorbia Fischeriana* Steud using Response Surface Methodology and Structure Identification by UPLC-Q-TOF-MS

Tiancheng Ma[a], Yu Sun[a *], Lei Liu[a], Jia Sun[a], Yukun Ma[a], Lina Guo[a] and Qi Liu[a]

[a]*Research Institute of Medicine and Pharmacy, Qiqihar Medical University, 161006 Qiqihar, China*

ABSTRACT

Jolkinolide A, jolkinolide B, 17-hydroxyjolkinolide A and 17-hydroxyjolkinolide B are abundant constitutes in *Euphorbia Fischeriana* Steud and exhibit profound bioactivities. In this study, they were selected as quality control to optimize the extraction of *E. fischeriana*. Response surface methodology employing Box-Behnken design was applied to test the optimal conditions for the extraction. The optimized conditions for the simultaneous extraction of four diterpenoids from *E. fischeriana* were: ethanol concentration 100%, extraction temperature 74℃ and extraction time 2.0 h. The extraction contents for jolkinolide A, jolkinolide B, 17-hydroxyjolkinolide A and 17-hydroxyjolkinolide B were 0.1763, 0.9643, 0.4245 and 2.8189 mg/g. The extract obtained under the optimal conditions was injected into UPLC-Q-TOF-MS system. Fifty-one peaks were identified. Two peaks were tentatively identified as new compounds. The compounds were diterpenoids, fatty oil, phenolics and others.

KEYWORDS:

Euphorbia Fischeriana Steud; efficient extraction; structure identification; diterpenoids; UPLC-Q-TOF-MS

Experimental

Chemicals and Reagents

The herbs of *E. fischeriana* (30 kg) were bought from Xianhe Pharmaceutical Company (Lot Number: 20160616) and verified as genuine ones according to China Pharmacopeia (2015 edition) by professor Lina Guo and Dezhi Ma of Qiqihar Medical University. Reference specimens and voucher specimens (1.0 kg) are kept in Research Institute of Medicine and Pharmacy of Qiqihar Medical University. The standards were prepared by ourselves. The purity of all standards were above 98.0%. Acetonitrile was purchased from Merck Company. Ethanol was purchased from Tianjin Fuyu chemical Co. Ltd. Formic acid was purchased from Tianjin commie chemical reagent Co. Ltd.

UPLC-MS detection

UPLC system (Shimadzu, Japan) consisted of a model LC-30AD pump and a model SIL-30AC autosampler. The chromatograph was equipped with a gradient mobile phase. Mobile phases were water with 0.1% of formic acid (A) and acetonitrile with 0.1% of formic acid (B). The gradient used was as follows: 0.01 min, 20% B; 0.01–1 min, 20% to 30% B; 1–7 min, 30% to 50% B; 7–10 min, 50% to 70% B; 10–15 min, 70% to 100% B; 15–16 min, 100%; 16–16.1 min, 100% to 20% B; 16.1–18 min, 100% B. The injection volume of sample was 1 μL. The flow rate was 0.3 $mL \cdot min^{-1}$ and the column temperature was 35℃. The Q-TOF-MS system (AB, America) with an ESI source was performed in positive mode and negative mode. The parameters of ESI-MS were set as follows: ion source gas 1 (50 psi), ion source gas 2 (50 psi), curtain gas (35 psi), temperature (500℃), ion spray voltage floating (5500 V), declustering potential (100 V), collision energy (10 V). MS conditions were corrected by APCI positive calibration solution for the AB SCIEX Triple TOF^{TM} systems.

Method validation

Linearity, LOD and LOQ

The linearity was established using a series of concentrations of standards. The calibration curves of the four compounds were constructed by plotting the integrated

chromatography peak areas (Y) versus the corresponding concentrations of the injected standard solutions (X) using a $1/x^2$ weighted linear least squares regression model. LOD and LOQ of the developed method for each compound were determined at signal-to-noise ratios (S/N) of 3 and 10 respectively.

Precision and recovery

The precision of the method was evaluated by intra-and inter-day variations. The extract was obtained under the optimized conditions. The sample was tested six times within a day for the intraday precision. The sample was analyzed in triplicate on three consecutive days for the inter day precision.

The accuracy of the method was verified by recovery tests. Spiked and unspiked samples were prepared to perform the recovery tests. Known amount of standard solutions were spiked into the root of *E. fischeriana*. Three concentration levels were prepared. The materials mixed with standards were extracted by optimized method for evaluating the accuracy. Precision and recovery were evaluated by relative standard deviations (RSDs).

Extraction procedure

Dried rhizomes of *E. fischeriana* were powdered by a disintegrator and then sieved into a homogeneous size (60 mesh). Extractions were carried out in water baths. The powders of 5.0 g were soaked in 100 mL different proportions of ethanol-water (from 0 % to 100%). Then, the heated reflux extraction experiments were conducted in water baths (from 20 to 100℃) for 0.5 to 2.5 h.

The filtered extraction solution (2 mL) with 50 μL internal standard fraxinellone (1 mg/mL) was to a 5 mL volumetric flask, dilute with acetonitrile to volume, and mix. Then, the mixture was filtered through 0.22 μm nylon membranes prior to UPLC analysis. The extraction was performed in triplicate.

Responses surface methodology

RSM was employed to determine the optimum levels of ethanol concentration (v/v, %) (X_1), extraction temperature (℃) (X_2) and extraction time (min) (X_3) related to responses yields of the contents of four diterpenoids. We evaluated the effects of ethanol concentration was ranged from 50 to 100%, ambient temperature that varied from 40 to 80℃, and the extraction time was evaluated from 1.0 to 2.0 h. All these conditions were selected based on preliminary experimental results. Moreover, BBD with RSM was applied to identify the best combination of the parameters. The effect

of three parameters on the extractions were investigated at three levels (-1, 0 and +1). In total, seventeen experiments were conducted in random order. The values were fitted with a second-order polynomial model given below:

$$Y = \beta_0 + \sum_{i=1}^{3} \beta_i X_i + \sum_{\mathrm{i}=1}^{3} \beta_{ii} X_i^2 + \sum_{\mathrm{i}=1}^{3} \sum_{\mathrm{j}=\mathrm{i}+1}^{3} \beta_{ij} X_i X_j$$

Where Y was the response; X_i and X_j were the independent variables influencing the response Y; β_0, β_i, β_{ii}, and β_{ij} described the regression coefficients for intercept, linear, quadratic and interaction terms, respectively. Design-Expert 8.0.6 was used to statistically analyzed the data. The quality of fit of the polynomial model was evaluated with respect to the coefficient of determination (R^2) and F-test. The lack of fit F-value ($P < 0.05$) was acquired by analysis of variance (ANOVA) and used to demonstrate variable significance and model adequacy.

Results

Investigation of the fragmentation patterns of reference standards

The extract obtained under the optimized conditions was injected into the UPLC-MS system.

To get the information about precursor ions and characteristic fragment ions of the compounds, jolkinolide A, jolkinolide B, 17-hydroxyjolkinolide A, 17-hydroxyjolkinolide B, euphopilolide, 12-deoxyphorbol-13-hexadecaoate, atis-16-en-13(S)-hydroxy-3,14-dione, ent-(16R)-16,17-dihydroxykauran-3-one and scopoletin were injected into the LC-MS system. The fragmentation patterns of the standards were discussed in detail below..

Jolkinolide A produced a precursor ion $[M+H]^+$ at *m/z* 315.1954 ($C_{20}H_{27}O_3$) with the retention time of 12.79 min. The ion at *m/z* 297.1846 was attributed to eliminate one molecule of water. The ion at *m/z* 269.1897 was produced by further loss of one molecule of carbonyl. The fragment ions at *m/z* 191.0706, 177.0551 and 163.0292 were attributed to skeleton residues by the cleavage of B-ring.

Jolkinolide B, 17-hydroxyjolkinolide A, 17-hydroxyjolkinolide B and euphopilolide are ent-abietane type diterpenoids, which produced $[M+H]^+$ ions at *m/z* 331.1901, 331.1904, 347.1844 and 317.2111 with the retention time of 11.70, 10.78, 9.75, 12.35 min. They produced ions which corresponded to residues by losses of water, carbonyl and cleavage of B-ring.

12-Deoxyphorbol-13-hexadecaoate gave $[M+H]^+$ ion at *m/z* 587.3964 with the

retention time of 16.68 min. It could generate ions at *m/z* 551.3772 and 331.1541, which corresponded to skeleton residues by losses of two molecules of water and hexadecaoate group at C-13. The fragment ions at *m/z* 313.1434, 303.1588 and 295.1321 were attributed to eliminate one molecule of water, one molecule of carbonyl and two molecules of water from 331.1541. The fragment ions at *m/z* 285.1485 and 267.1390 were attributed to eliminate two molecules of water from 303.1588. The fragment ions at *m/z* 257.1523 and 239.1421 were attributed to skeleton residues by the cleavage of B-ring.

Atis-16-en-13(S)-hydroxy-3,14-dione produced $[M+H]^+$ ion at *m/z* 317.2096 with the retention time of 6.56 min. The fragment ions at *m/z* 299.1995, 281.1888 and 263.1781 were attributed to successive losses of three molecules of water. The fragment ions at *m/z* 289.2156, 271.2048 and 253.1946 were attributed to successively eliminate one molecule of carbonyl and two molecules of water. The fragment ions at *m/z* 257.1891 and 229.1575 were attributed to skeleton residues by the cleavage of C-ring.

Ent-(16R)-16,17-dihydroxykauran-3-one showed $[M+H]^+$ ion at *m/z* 321.2426 with the retention time of 6.77 min. It produced ions at *m/z* 303.2318, 285.2211 and 267.2108, which were attributed to the sequential losses of three molecules of water. The fragment ion at *m/z* 257.2258 was attributed to losses of two molecules of H_2O and CO. The fragment ion at *m/z* 227.1793 was attributed to loss of one molecule of water and cleavage of C-ring.

Scopoletin showed $[M+H]^+$ ion at *m/z* 193.0504 with the retention time of 2.88 min. It produced ions at *m/z* 178.0268 and 150.0312 were attributed to the sequential losses of $\cdot CH_3$ and carbonyl. The fragment ion at *m/z* 133.0283 was attributed to the losses of CH_3OH and CO. The fragment ion at *m/z* 105.0333 was attributed to the loss of H_2O and cleavage of B-ring.

Investigation of the structures of diterpenoids in E. fischeriana

Fifty-one peaks were identified based on comparison of retention times, accurate masses and fragmentation patterns with available standard compounds and literatures (Table S1). They were diterpenoids, fatty oil, phenolics and others. Diterpenoids were classified into 7 subtypes, namely, ent-abietane type diterpenoids, tigliane type diterpenoids, ent-atisane type diterpenoids, daphnane type diterpenoids, lathyrane type diterpenoids, diterpene lactone and sesterpenoid.

It is supposed that peaks 9, 13, 15, 24, 25, 27, 30, 31, 32, 33, 34, 35, 36, 37, 40, 41, 42 and 46 were ent-abietane type diterpenoids. Peaks 31, 36, 40, 41 and 42 were identified as 17-hydroxyjolkinolide B, 17-hydroxyjolkinolide A, jolkinolide B, jolkinolide A and euphopilolide according to authentic standards. Peak 9 produced $[M+H]^+$ ion at *m/z* 347.1846 with the retention time of 3.94 min. It produced ion at *m/z* 329.1760, 311.1625 and 265.1609, which were attributed to the sequential losses of two molecules of water and one molecule of HCOOH. The fragment ion at *m/z* 287.1588 was attributed to the sequential losses of CO and CH_3OH. The fragment ions at *m/z* 173.0977 and 159.0441 were attributed to the cleavage of A-ring. It was tentatively identified as 11α,17-dihydroxyhelioscopinolide E (Wang et al. 2017). The molecular masses of peaks 13 and 15 were 58 Da heavier than those of jolkinolide B and jolkinolide A. Peak 13 presented $[M+H]^+$ ion with mass accuracy at *m/z* 389.1959 at the retention time with 4.74 min. It produced fragment ions at *m/z* 311.1591 and 293.1576, which were attributed to the sequential losses of CH_3COOH, one molecule of water and another molecule of water. The fragment ion at *m/z* 283.1630 was attributed to the losses of CH_3COOH, CO and one molecule of water from *m/z* 389.1959. The fragment ion at *m/z* 237.1266 was attributed to the cleavage of D-ring. It was tentatively identified as 17-acetoxyjolkinolide B (Wang et al. 2017). Peak 15 presented $[M+H]^+$ ion at *m/z* 373.2010 at the retention time of 5.30 min. It produced fragment ions at *m/z* 313.1796, 295.1684 and 277.1586, which were attributed to the sequential losses of CH_3COOH and two molecules of water. The fragment ion at *m/z* 267.1741 was corresponded to the sequential losses of CH_3COOH, H_2O and CO. The fragment ion at *m/z* 255.1263 was attributed to the cleavage of D-ring. It was tentatively identified as 17-acetoxyjolkinolide A (Che et al. 2017). Peak 24 presented $[M+H]^+$ ion with mass accuracy at *m/z* 351.2163 at the retention time of 7.11 min. It produced fragment ions at *m/z* 333.2078, 315.1956 and 297.1846, which were attributed to the sequential losses of three molecules of water. The fragment ions at *m/z* 287.1978 and 269.1830 were attributed to the losses of HCOOH and water from *m/z* 333.2078. It was tentatively identified as yuexiandajisu E (Wang et al. 2013). Peak 25 presented $[M+H]^+$ ion with mass accuracy at *m/z* 351.2153 at the retention time of 7.80 min. It produced samilar fragment ions as peak 24. It was tentatively identified as yuexiandajisu D (Lee et al. 2016). Peak 27 showed $[M+H]^+$ ion at *m/z* 349.2002 with the retention time of 8.45 min. It produced ions at *m/z* 331.1912, 313.1810 and 295.1707, which were attributed to losses of three molecules of water.

The fragment ions at *m/z* 285.1846 and 267.1729 were attributed to the losses of CO and HCOOH from *m/z* 313.1810. The ions at *m/z* 175.0379 and 147.0435 were attributed to the cleavage of rings. It was tentatively identified as 7β,11β,12β-trihydroxy-ent-abieta-8(14),13(15)-dien-16,12-olide. Peaks 24 and 25 were 16 Da heavier than that of peak 30. Peak 30 showed $[M+H]^+$ ion at *m/z* 335.2210 with the retention time of 9.36 min. It produced ions at *m/z* 317.2020, 289.1411 and 253.1903, which were attributed to losses of one molecule of water, HCOOH and another two molecules of water from *m/z* 335.2210. It was tentatively identified as 8β,14α-dihydroxyabiet-13(15)-ene-16,12-lactone (Yan et al. 2008). Peak 35 showed $[M+H]^+$ ion at *m/z* 363.2161 with the retention time of 10.59 min. It produced ions at *m/z* 345.2058, 331.1881 and 317.2070, which were attributed to losses of one molecule of water, CH_3OH and CH_3COOH. The ions at *m/z* 295.1754, 285.1827, 267.1733 and 257.1934 were attributed to sequential losses molecules of water and carbonyls from *m/z* 331.1881. It was tentatively identified as euphorin H (Kuang et al. 2016). Peak 34 showed $[M+H]^+$ ion at *m/z* 329.2116 with the retention time of 10.56 min. Similar as peak 35, it produced ions at *m/z* 297.1840 and 269.1908, which were attributed to losses of CH_3OH and CH_3COOH. The ion at *m/z* 241.1211 was attributed to loss one molecule of CO from *m/z* 269.1908. It produced a series of fragment ions which were attributed to the ions of cleavage of rings. It was tentatively identified as a new compound named (Z)-methyl 2-((4bR,8aR)-4b,8,8-trimethyl -3-oxo-4b,5,6,7,8,8a,9,10-octahydrophenanthren-2(3H)-ylidene)propanoate. Peak 37 exhibited $[M+H]^+$ ion at *m/z* 317.2111 with the retention time of 11.00 min. It produced ions at *m/z* 299.1997, 289.2139, 281.1890 and 271.2050 which were attributed to the losses of molecules of water and carbonyls. The ion at *m/z* 253.1925 was attributed to the loss of HCOOH from 299.1997. It was tentatively identified as ent-11β-hydroxyabieta-8(14),13(15)-dien-16,12β-olide (Kuang et al. 2016). The molecular masses of peaks 32 and 33 were 16 Da heavier than that of peak 37 with the retention time of 9.99 and 10.17 min. They showed similar fragment ions. They were tentatively identified as fischeriolide A and fischeriolide C. Peak 46 showed $[M+H]^+$ ion at *m/z* 315.1955 with the retention time of 12.73 min. It produced ions at *m/z* 297.1841 and 269.1910 which were attributed to losses of water and HCOOH. The fragment ions at *m/z* 191.0698, 177.0546, 163.0383, 149.0593 and 139.0384 were attributed to the cleavage of rings. It was tentatively identified as a new compound, which named (1aR,7aR,11aR,11cR)-4,8,8,11a-tetramethyl-

6,7,7a,8,9,10,11,11a,11b,11c-decahydro-3H-oxireno[2',3':3,4]phenanthro[3,2-b]furan-3-one.

Peaks 14, 20, 21, 23, 26, 29, 38, 45, 48, 49 and 50 were tentatively identified as ent-atisane type diterpenoids. Peaks 20 and 23 were identified as atis-16-en-13(S)-hydroxy-3,14-dione and ent-(16R)-16,17-dihydroxykauran-3-one according to authentic standards. Peak 45 was 30 Da less than that of peak 23. Peak 45 produced ion at *m/z* 245.2274, which was attributed to the loss of carbonyl and the cleavage of C ring. It was tentatively identified as ent-kaurane-3-oxo-16α,17-diol (Liang et al. 2014). Peak 48 was 16 Da less than that of peak 20. Peak 48 showed $[M+H]^+$ ion at *m/z* 301.2161 with the retention time of 13.85 min. It produced ions at *m/z* 283.2042 and 255.2103, which were attributed to the losses of water and carbonyl. The ions at *m/z* 173.1328 and 145.0648 were attributed to the cleavage of rings. It was tentatively identified as ent-atis-16(17)-ene-3,14-dione (Yang et al. 2011). Peak 14 showed $[M+H]^+$ ion at *m/z* 337.2368 with the retention time of 4.76 min. It produced ions at *m/z* 319.2301, 301.2161 and 283.2040, which were attributed to the sequential losses of three molecules of water. The fragment ion at *m/z* 253.1962 was corresponded to the cleavage of $-CH_2OH$ on C-ring from 283.2040. The fragment ion at *m/z* 225.1630 was attributed to the cleavage of C-ring. It was tentatively identified as 3S,16S,17-trihydroxy-2-one-ent-kaurane. Peak 49 showed $[M+H]^+$ ion at *m/z* 323.2580 with the retention time of 14.49 min. Peak 49 was 14 Da less than that of peak 14. It was tentatively identified as ent-atisane-3β,16α,17-triol (Lee et al. 1991). Peak 21 showed $[M+H]^+$ ion at *m/z* 303.2297 with the retention time of 6.75 min. It produced ions at *m/z* 285.2185, 267.2086 and 257.2310, which were attributed to the losses of molecules of water and carbonyl. The fragment ions at *m/z* 227.1830, 215.1421, 213.1600, 211.1501, 185.1335 and 183.1146 were attributed to the cleavage of rings. It was tentatively identified as ent-(3α,5β,8α,9β,10α, 12α)-3-hydroxyatis-16-en-14-one. Peak 26 showed $[M+H]^+$ ion at *m/z* 317.2103 with the retention time of 6.95 min. It produced ions at *m/z* 299.1978 and 281.1913, which were attributed to the losses of two molecules of water. The fragment ion at *m/z* 271.2058 was attributed to losses of one molecule of water and CO. The fragment ion at *m/z* 257.1873 was attributed to the cleavage of rings. It was tentatively identified as ent-3β-hydroxyatis-16-ene-2,14-dione. Peak 38 was 16 Da heavier than that of peak 20. Peak 38 produced ions at *m/z* 301.2125 and 199.1479, which were attributed to the losses of molecule of water and the cleavage of rings. It was tentatively identified as ent-3β,(13S)-dihydroxyatis-16-

en-14-one (Liang et al. 2014). Peak 29 showed $[M+H]^+$ ion at *m/z* 335.2211 with the retention time of 9.14 min. It produced ions at *m/z* 317.2093, 299.1909 and 271.2069, which were attributed to the sequential losses of three molecules of water. The fragment ions at *m/z* 215.1417, 203.1035, 145.1016, 133.0650 and 119.0843 were attributed to the cleavage of rings. It was tentatively identified as alboatisin A (Yang et al. 2011). Peak 50 showed $[M+H]^+$ ion at *m/z* 289.2514 with the retention time of 15.63 min. It produced ions at *m/z* 271.2406 and 233.1903 which were attributed to the sequential losses of water and cleavage of ring. It was tentatively identified as ent-kaur-16-en-14-ol (Wang et al. 2012).

Peaks 3, 10, 22, 39 and 51 were tentatively identified as tigliane type diterpenoids. Peak 51 was identified as 12-deoxyphorbaldehyde-13-hexadecanoate according to the authentic standard. Peak 3 showed $[M+H]^+$ ion at *m/z* 569.2590 with the retention time of 1.73 min. It produced ions at *m/z* 389.1865, 371.1815, 353.1766 were attributed to sequential losses of one molecule of water, glycosyl and two molecules of water. The ions 329.1754, 311.1634, 293.1542, 275.1418 and 265.1566 were attributed to losses of acetyl, molecules of water and carbonyl. It was tentatively identified as fischeroside C. Peak 3 was 16 Da heavier than that of peak 10. Peak 10 showed $[M+H]^+$ ion at *m/z* 553.2637 with the retention time of 4.09 min. It produced a series of ions attributed to losses of acetyl, molecules of water and glycosyl. It was tentatively identified as fischeroside A (Wang et al. 2017). Peak 22 showed $[M+H]^+$ ion at *m/z* 405.1941 with the retention time of 6.75 min. It produced ions at *m/z* 387.1769 and 341.1762 were attributed to losses of one molecule of water and HCOOH. It was tentatively identified as 20-oxo-prostratin. Peak 39 showed $[M+H]^+$ ion at *m/z* 391.2117 with the retention time of 11.58 min. It produced ion at *m/z* 281.1527 was attributed to losses of CH_3COOH, H_2O and CH_3OH. The ion at *m/z* 215.0732 was generated by the cleavage of C-ring. It was tentatively identified as prostratin (Wang et al. 2010).

Peak 6, 17 and 19 were tentatively identified as daphnane type diterpenoids. Peak 6 showed $[M+H]^+$ ion at *m/z* 511.2527 with the retention time of 2.40 min. The produced ions at *m/z* 331.0475, 313.1805, 295.1762, 285.1814, 267.1712 and 257.1173 were attributed to the sequential losses of glycosyl, molecules of water and carbonyls. It was tentatively identified as euphopiloside A (Wei et al. 2018). Peak 17 showed $[M+H]^+$ ion at *m/z* 347.1852 with the retention time of 6.10 min. It produced ions at *m/z* 329.1739, 311.1644 and 283.1672, which were attributed to the sequential

losses of three molecules of water. The fragment ion at *m/z* 213.0899 was attributed to the cleavage of A-ring. It was tentatively identified as (3aR,6aS,10R,10aR,10bS)-3a,10a-dihydroxy-5-(hydroxymethyl)-2,10-dimethyl-7-(propan-2-ylidene)-3a,4,6a,7,10,10a-hexahydrobenzo[e]azulene-3,8(9H,10bH)-dione. Peak 19 presented $[M+H]^+$ ion at *m/z* 347.1847 at the retention time of 6.54 min. The fragment ions at *m/z* 329.1743, 283.1718, 311.1615 were attributed to losses of three molecules of water. The fragment ion at *m/z* 301.1615 was attributed to the sequential losses of CO and H_2O. The fragment ion at *m/z* 241.0880 was attributed to the cleavage of A-ring. It was tentatively identified as (3aR,6aS,7R,10R,10aR,10bS)-3a,10a-dihydroxy-5-(hydroxymethyl)-2,10-dimethyl-7-(prop-1-en-2-yl)-3a,4,6a,7,10,10a-hexahydrobenzo[e]azulene-3,8(9H,10bH)-dione (Wang et al. 2010).

Peak 28 was tentatively identified as lathyrane type diterpenoids. It showed $[M+H]^+$ ion at *m/z* 481.2590 with the retention time of 9.01 min. It produced fragment ions at *m/z* 315.1964, 287.2051 and 269.1912, which were attributed to the sequential losses of water, cinnamic acid, carbonyl and water. The fragment ion at *m/z* 297.1839 was corresponded to the cleavage of ring. It was tentatively identified as jolkinol A (Lee et al. 2016).

Peak 43 was tentatively identified as diterpene lactone. It showed $[M+H]^+$ ion at *m/z* 289.2513 with the retention time of 12.40 min. The produced ions at *m/z* 271.2044 and 233.1874 were attributed to the sequential losses of one molecule of water and lactonic ring. The fragment ion at *m/z* 109.1003 was attributed to the cleavage of C ring. It was tentatively identified as fischeria A (Kuang et al. 2016).

Peak 44 was tentatively identified as sesterterpenoid. It showed $[M+H]^+$ ion at *m/z* 525.2115 with the retention time of 12.47 min. The produced ions at *m/z* 481.2216, 463.2119, 445.2035 and 439.2094 were attributed to the sequential losses of ester group, two molecules of water and acetyl. The fragment ion at *m/z* 275.0557 was attributed to the cleavage of ring and losses of carbonyl. It was tentatively identified as langduin D (Pan et al. 2011).

Investigation of the structures of phenolics and fatty acid in E. fischeriana.

Peaks 1, 2, 4, 5, 7, 8, 11, 12, 16 and 18 were tentatively identified as phenolics. Peaks 1 and 2 produced $[M+NH_4]^+$ ions at *m/z* 654.1276 and 654.1280 with the retention time of 1.16 and 1.44 min. They showed similar fragment ions. The fragment ions at *m/z* 619, 449, 279 and 109 were attributed to the losses of one molecule of water and three molecules of gallic acid. They were tentatively identified

as 1,3,6-tri-O-galloyl-β-D-allopyranose and 1,2,6-tri-O-galloyl-β-D-allopyranose (Wang et al. 2016). Peaks 4 and 5 presented $[M+H]^+$ ions at *m/z* 477.1603 and 491.1168 with the retention time of 1.88 and 2.23 min. They produced fragment ions, which were attributed to the sequential losses of glycosyls and water. They were tentatively identified as 2,4-dihydroxy-6-methoxyacetophenoe-4-O-α-L-arabinofuranosyl(1→6)-β-D-glucopyranoside and 2,4-dihydroxy-6-methoxyacetophenoe-5-methyl-4-O-α-L-rhamnosyl (1→6)-β-D-glucopyranoside (Huang et al. 2017). Peak 7 presented $[M+H]^+$ ion with mass accuracy at *m/z* 345.1176 ($C_{15}H_{21}O_9$) at the retention time of 2.45 min. It produced fragment ions at *m/z* 183.0645, 165.0544 and 137.0593, which were attributed to the sequential losses of one molecule of hexose residue, one molecule of water and one molecule of methoxy group. Based on the fragment ions, it was tentatively identified as 2,4-dihydroxy-6-methoxyacetophenoe 4-O-β-D-glucopyranoside. Peak 8 was identified as scopoletin according to the authentic standard. Peaks 11 and 18 produced $[M+H]^+$ ions at *m/z* 331.0444 and 345.0608 with the retention time of 4.52 and 6.18 min. They produced fragment ions, which were attributed to the sequential losses of methoxyl and water. They were tentatively identified as 3,8-dihydroxy-2,7-dimethoxychromeno[5,4,3-cde]chromene-5,10-dione and 3-hydroxy-2,7,8-trimethoxychromeno[5,4,3-cde]chromene-5,10-dione (Cui et al. 2017). Peaks 12 and 16 presented $[M+H]^+$ ions with mass accuracy at *m/z* 183.0653 and 197.0808 with the retention time of 4.57 and 5.92 min. They produced fragment ions, which were attributed to the sequential losses of water, methoxyl and hydroxyl. They were tentatively identified as 1-(2,4-dihydroxy-6-methoxyphenyl)ethanone and 3-acetyl-2,6-dihydroxy-4-methoxybenzaldehyde (Lee et al. 2016).

Peak 47 produced $[M+H]^+$ ions at *m/z* 279.2316 with the retention time of 13.82 min. It was tentatively identified as α-linolenic acid. As fatty acid, it produced a series of ions losses of methyl and methylene (Wang et al. 2012).

Discussion

In the single-factor experiments, ethanol concentration and the extraction temperature had more remarkable effects on the extraction yields. The amounts of the extracted target diterpenoids increased with the increase of ethanol concentration. The extraction yields of jolkinolide B, 17-hydroxyjolkinolide A and 17-hydroxyjolkinolide B were less when temperature was too high.

The extract along with 9 standards were injected into UPLC-Q-TOF-MS system. Data were obtained using Analyst TF 1.7.1 Software. PeakView was applied to analyze the data. In order to identify the structures, compound library was established by ourselves. More than eighty compounds of *E. fischeriana* were collected from literatures. MasterView was used to simulated the fragmentation pattern of each compound, which would raise the reliability of the results. TCM MS/MS Library was applied to predict the potential compounds. Both positive and negative ion modes were tested. It showed that the analyses obtained with the positive ion mode exhibited greater responses to fragments. According to the results, diterpenoids were the main constituents of *E. fischeriana*. Determining the key fragment ions and possible fragmentation patterns of standards would be beneficial for identifying other diterpenoids. Neutral losses like H_2O, CO, HCOOH, CH_3OH and CH_3COOH, cleavages of ring A, ring B, ring C and the lactonic ring were responsible for the main fragmentation patterns of diterpenoids. In MSMS spectrogram, ent-abietane type diterpenoids usually showed cleavages of ring A, ring B and the lactonic ring. Cleavage of ring C often could be seen in ent-atisane type diterpenoids. Diterpene lactone exhibited the cleavage of lactonic ring. Sugar residues and fatty chains were likely to lose when they were attached to diterpenoids. However, the structures of diterpenoids are complex, the analytical method has some limitations in identifying the isomers. To confirm the structures of the compounds, NMR experiments are necessary.

References

Che CT, Zhou TX, Ma QG, Qin GW, Williams ID, Wu HM. 2017. Diterpenes and aromatic compounds from *Euphorbia fscheriana*. Phytochemistry. 52: 117-121.

Cui J, Yang X, Dong AJ, Cheng DY, Wang J, Zhao HT. 2011. Chemical composition and antioxidant activity of *Euphorbia fischeriana* essential oil from China. J Med Plants Res. 5: 4794-4798.

Huang SS, Li P, Zhang BJ, Deng S, Zhang HL, Sun CP. 2017. Acetophenone glycosides from the roots of *Euphorbia fischeriana* and their inhibitory effects against Mycobacterium smegmatis. Phytochem Lett. 19: 151-155.

Kuang XZ, Li W, Kanno Y, Yamashita N, Kikkawa S, Azumaya I. 2016 Euphorins A-H, bioactive diterpenoids from Euphorbia fischeriana. J Nat Med. 70: 412-422.

Lee JW, Lee C, Jin Q, Jang H, Lee D, Lee HJ. 2016. Diterpenoids from the Roots of

Euphorbia fischeriana with Inhibitory Effects on Nitric Oxide Production. J Nat Prod. 79: 126-131.

Lee SH, Tanaka T, Nonaka G, Nishioka I, Zhang B. 1991. Allose gallates from *Euphorbza Fischeriana*. Phytochemistry. 30: 1251-1253.

Liang X, Liu ZG, Cao YF, Meng DL, Hua HM. 2014. Chemotaxonomic and chemical studies on two plants from genus of Euphorbia, Euphorbia fischeriana and Euphorbia ebracteolata. Biochem Syst Ecol. 57: 345-349.

Pan LL, Fang PL, Zhang XJ, Ni W, Li L, Yang LM. 2011. Tigliane-type diterpenoid glycosides from Euphorbia fischeriana. J Nat Prod. 74: 1508-1512.

Wang CJ, Yan QL, Ma YF, Sun CP, Chen CM, Tian XG. 2017. ent-Abietane and tigliane diterpenoids from the roots of Euphorbia fischeriana and their inhibitory effects against mycobacterium smegmatis. J Nat Prod. 80: 1248-1254.

Wang HB, Chen W, Zhang YY, Wang XY, Liu LP, Tong LJ. 2013. Four new diterpenoids from the roots of *Euphorbia fischeriana*. *Fitoterapia*. 91: 211-216.

Wang HB, Chu WJ, Wang Y, Ji P, Wang YB, Yu Q. 2010. Diterpenoids from the roots of Euphorbia fischeriana. J Asian Nat Prod Res. 12: 1038-1043.

Wang M, Wang QH, Wei Q, Li J, Guo C, Yang BY. 2016. Two new ent-atisanes from the root of Euphorbia fischeriana Steud. Nat Prod Res. 30: 144-149.

Wang XY, Liu LP, Kang TG, Wang HB. 2012. Chemical constituents of Euphorbia fischeriana. Chin J Nat Med. 10: 299-302.

Wei YL, Yu ZL, Huo XK, Tian XG, Feng L, Huang SS. 2018. Diterpenoids from the roots of *Euphorbia fischeriana* and their inhibitory effects on alpha-glucosidase. J Asian Nat Prod Res. 20: 977-984.

Yang LB, Liu SJ, Zhang B, Suo YR. 2011. Alboatisin A, a new diterpenoid from *Euphorbia fischeriana*. J Chem Res. 35: 692-693.

Yan SS, Li Y, Wang Y, Shen SS, Gu Y, Wang HB. 2008. 17-Acetoxyjolkinolide B irreversibly inhibits IkappaB kinase and induces apoptosis of tumor cells. Mol Cancer Ther. 7: 1523-1532.

Figures

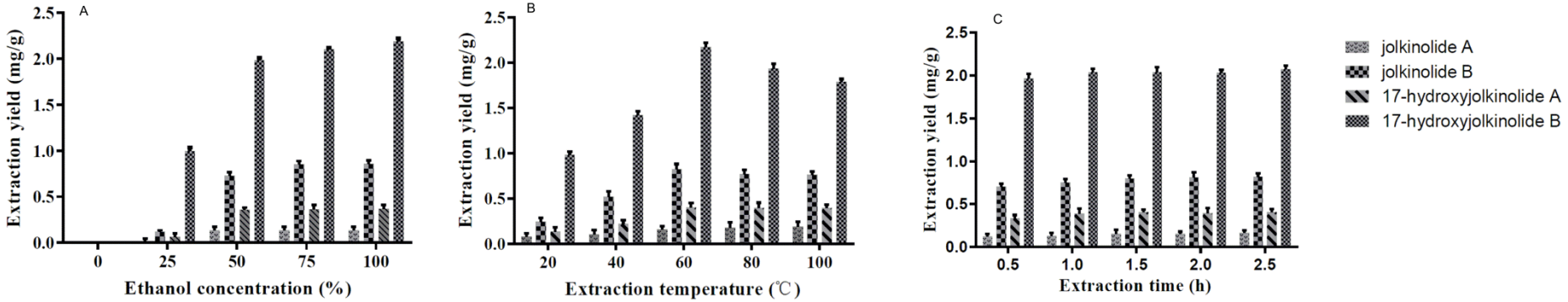

Figure S1. Effect of ethanol concentration (A), extraction temperature (B) and extraction time (C) on the extraction yield of jolkinolide A, jolkinolide B, 17-hydroxy jolkinolide A and 17-hydroxy jolkinolide B

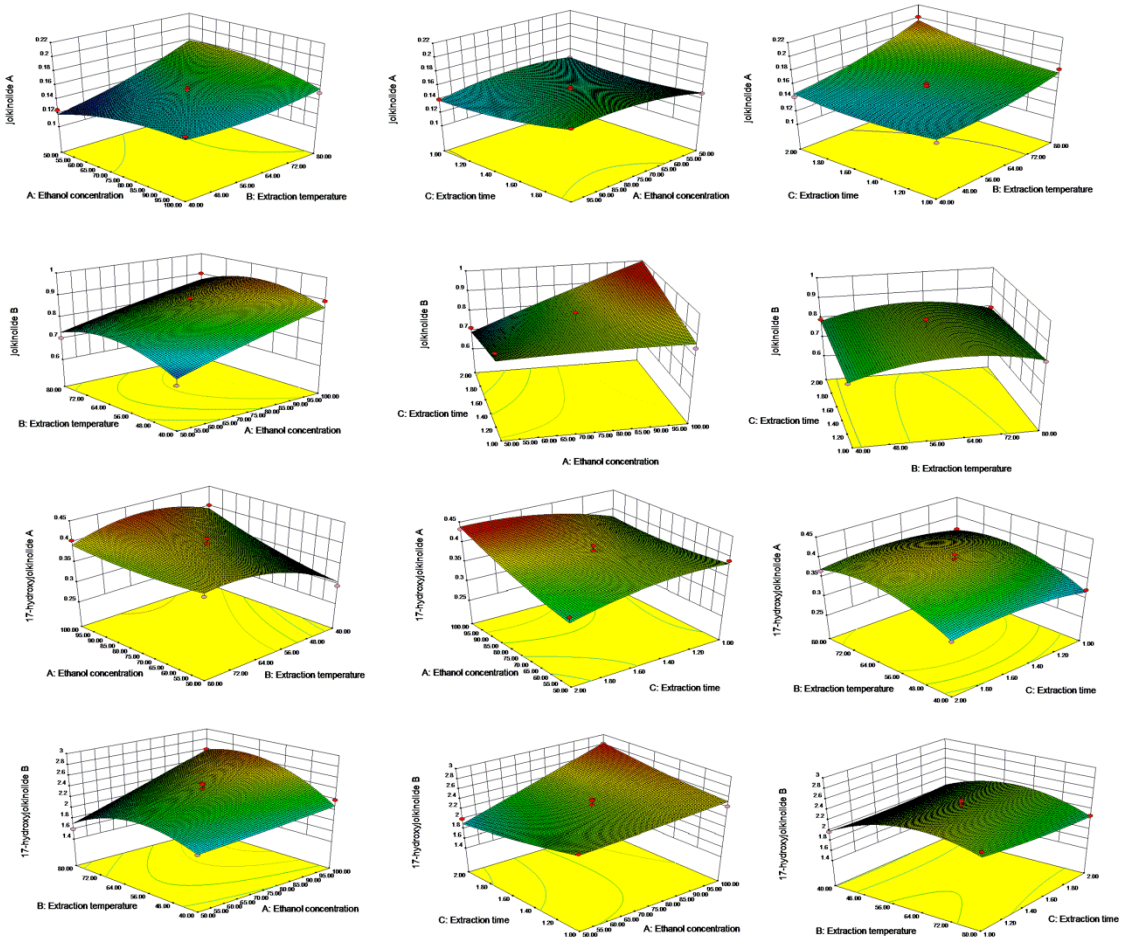

Figure S2. Response surface plots (3D) of the extraction yield of jolkinolide A, jolkinolide B, 17-hydroxy jolkinolide A and 17-hydroxy jolkinolide B of significant interactions between factors: ethanol concentration (A), extraction time (B) and extraction temperature (C)

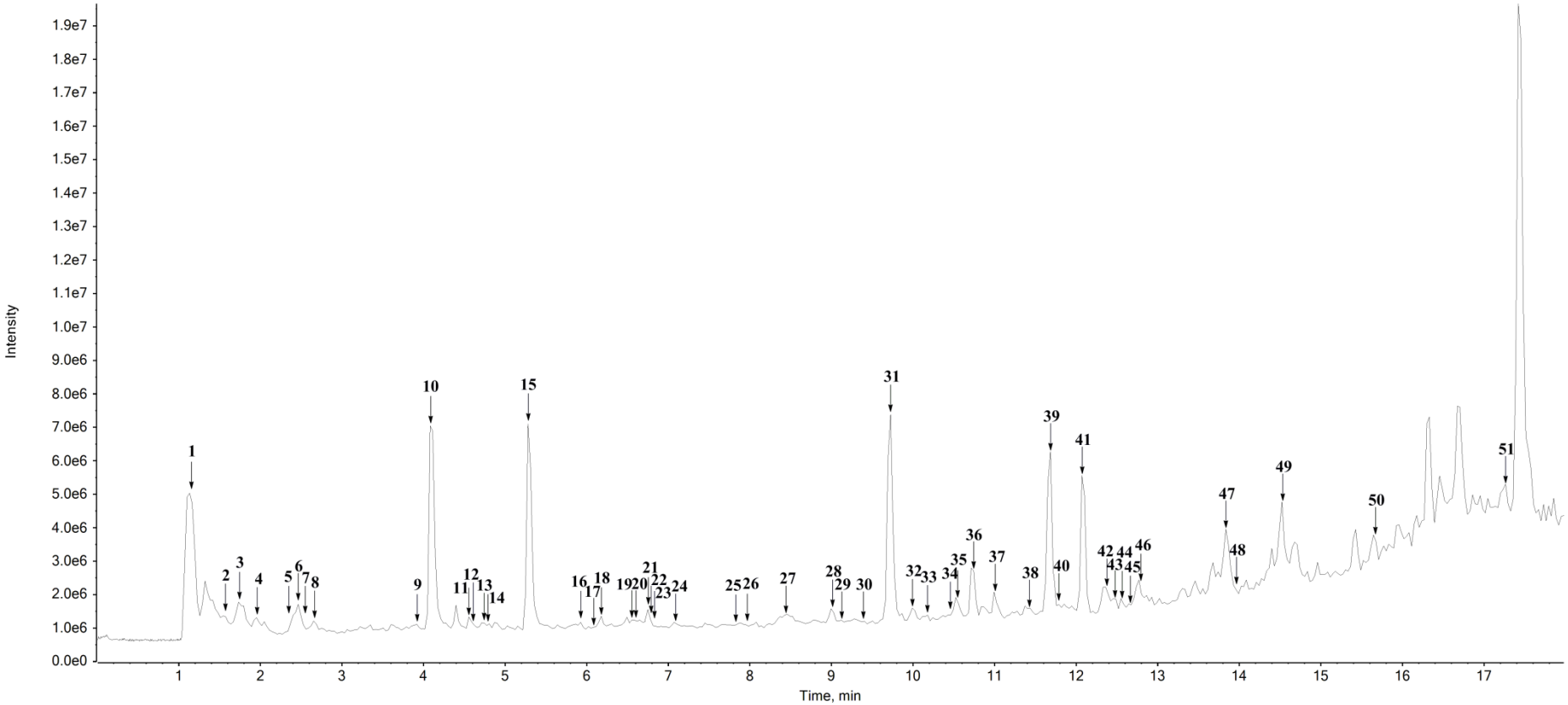

Figure S3. Total ion chromatogram of the extraction of *E. fischeriana*

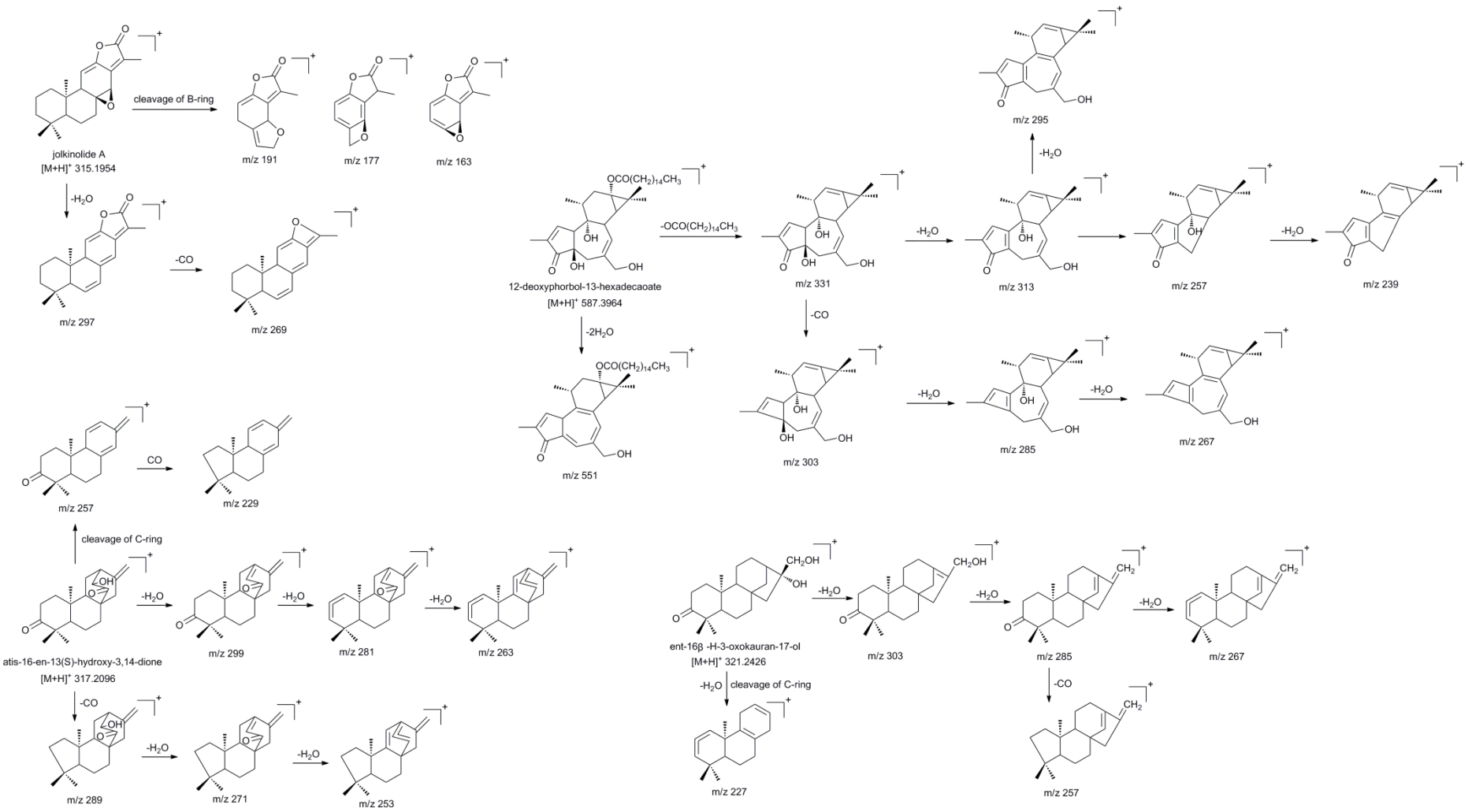

Figure S4. Fragmentation patterns of representative standards

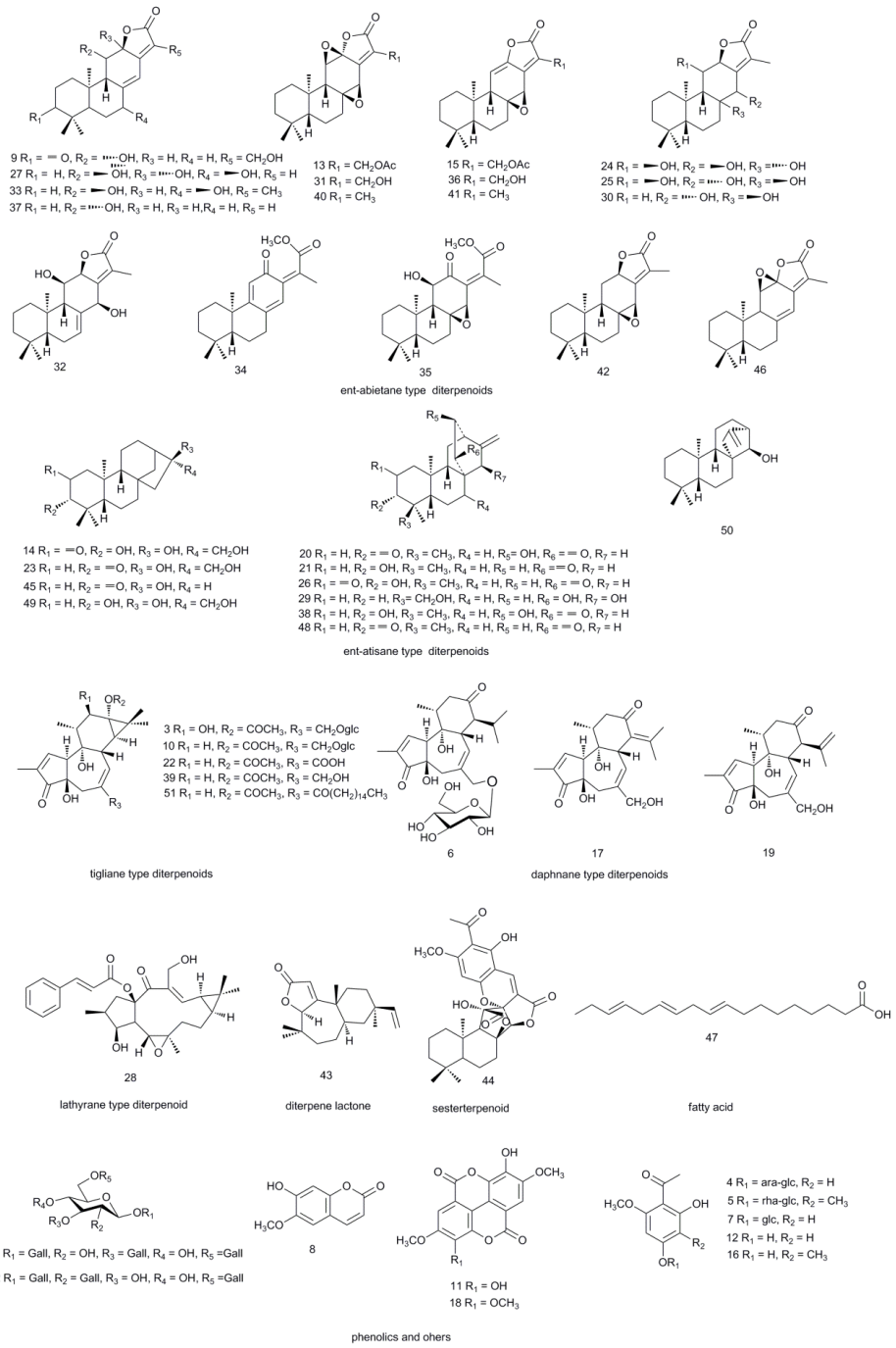

Figure S5. Structures of compounds from *E. fischeriana*

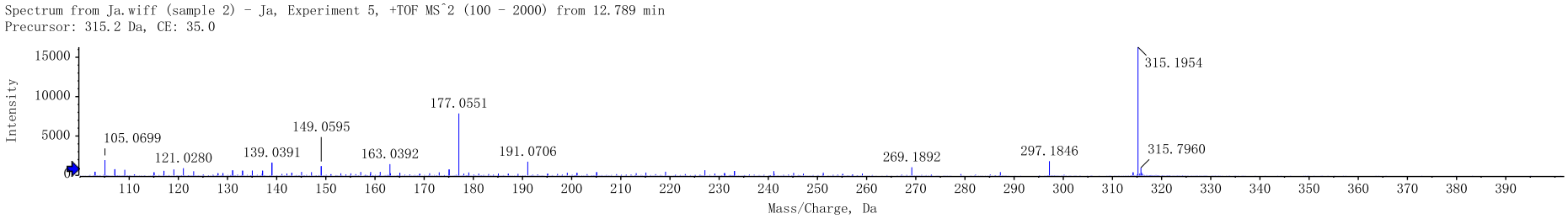

Figure S6. MSMS spectrogram of jolkinolide A

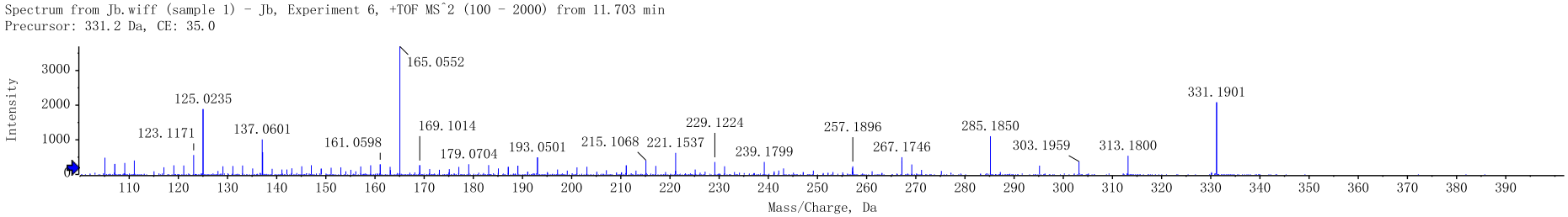

Figure S7. MSMS spectrogram of jolkinolide B

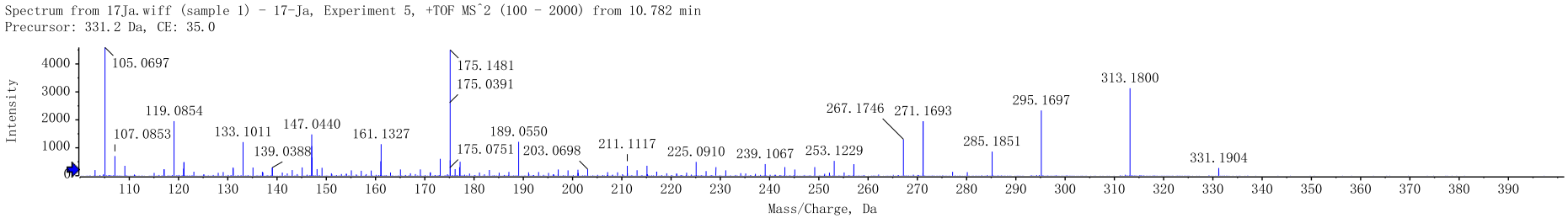

Figure S8. MSMS spectrogram of 17-hydroxyjolkinolide A

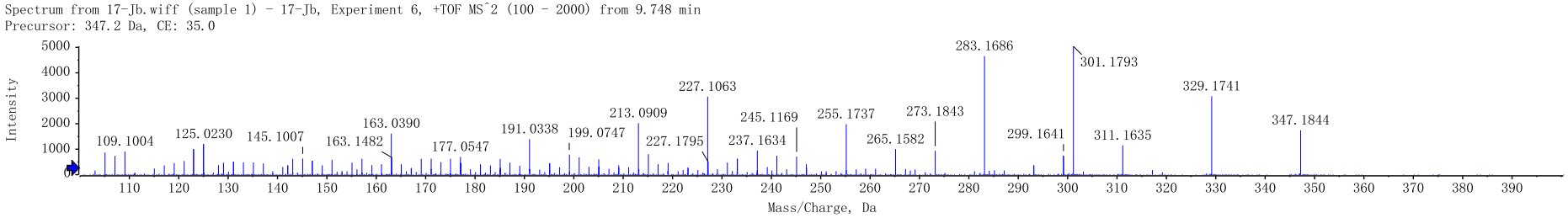

Figure S9. MSMS spectrogram of 17-hydroxyjolkinolide B

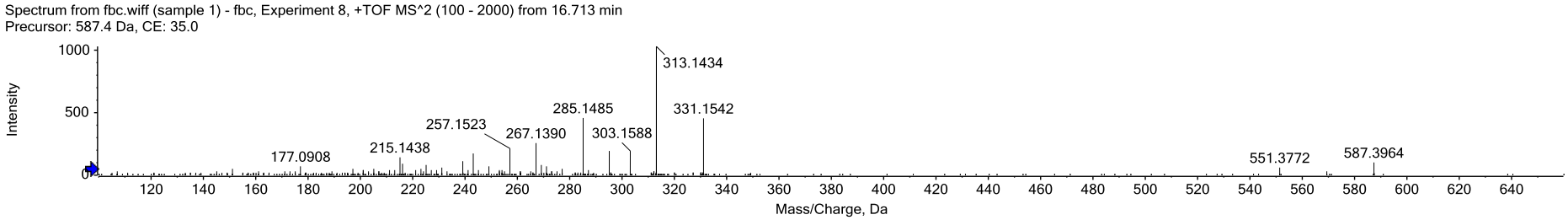

Figure S10. MSMS spectrogram of 12-deoxyphorbol-13-hexadecaoate

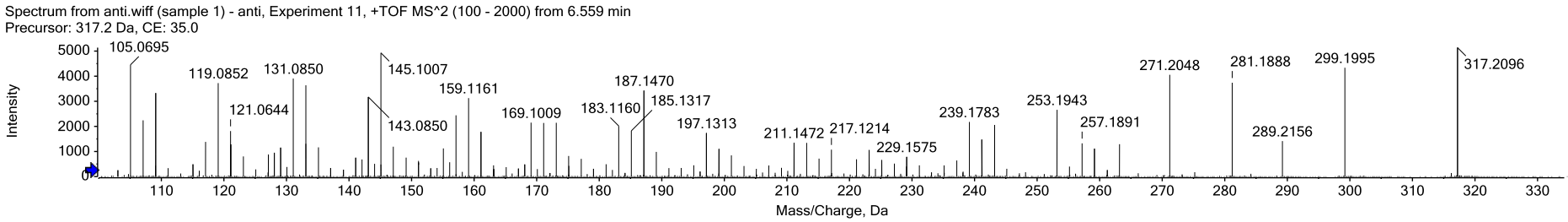

Figure S11. MSMS spectrogram of atis-16-en-13(S)-hydroxy-3,14-dione

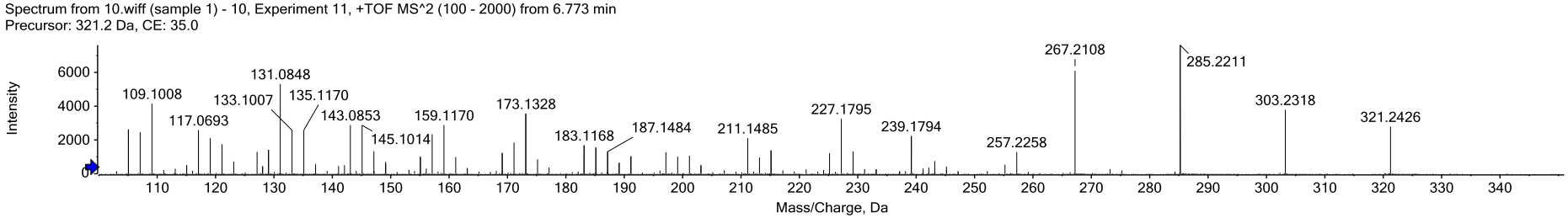

Figure S12. MSMS spectrogram of ent-(16R)-16,17-dihydroxykauran-3-one

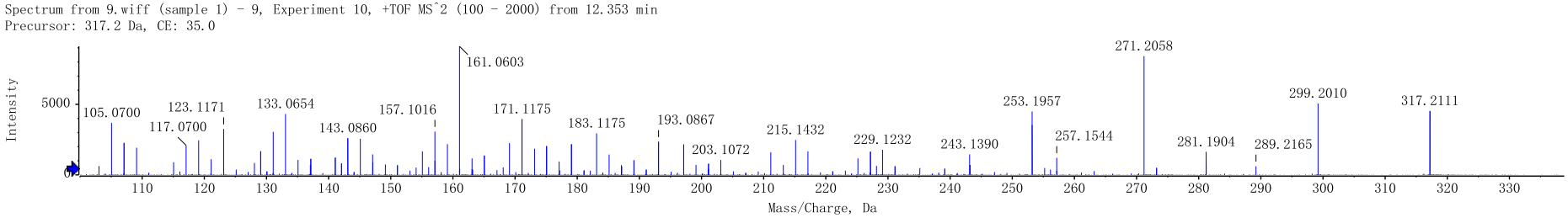

Figure S13. MSMS spectrogram of euphopilolide

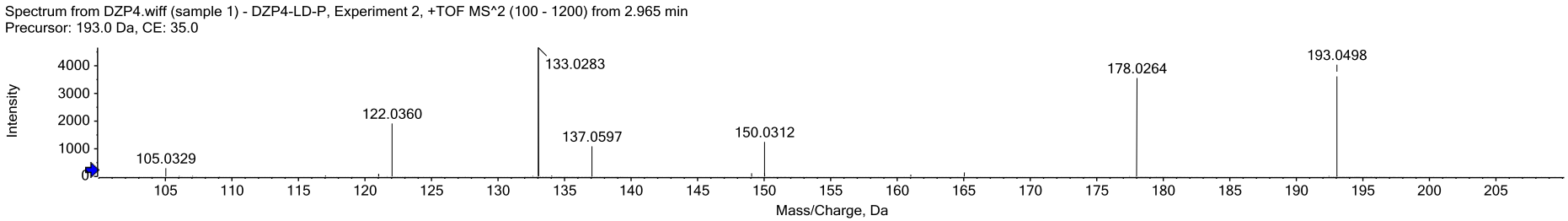

Figure S14. MSMS spectrogram of scopoletin

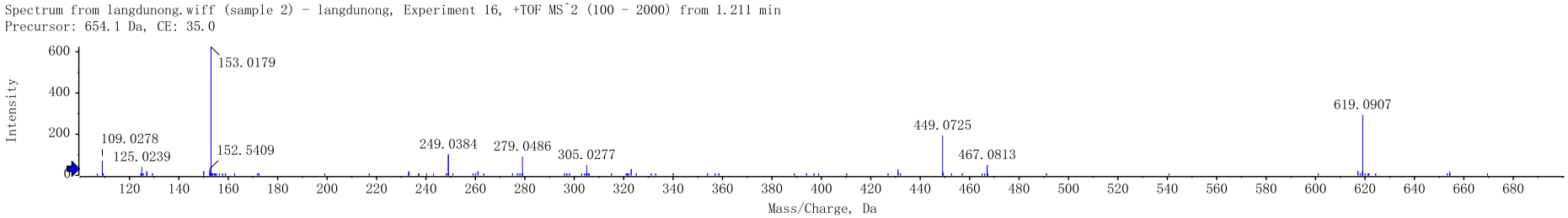

Figure S15. MSMS spectrogram of peak 1

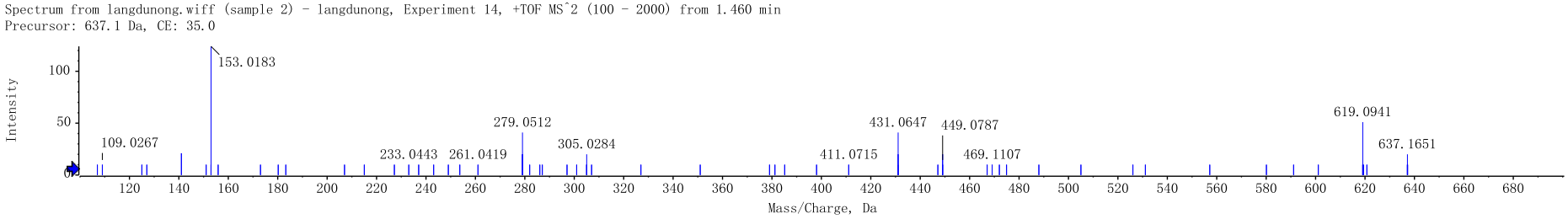

Figure S16. MSMS spectrogram of peak 2

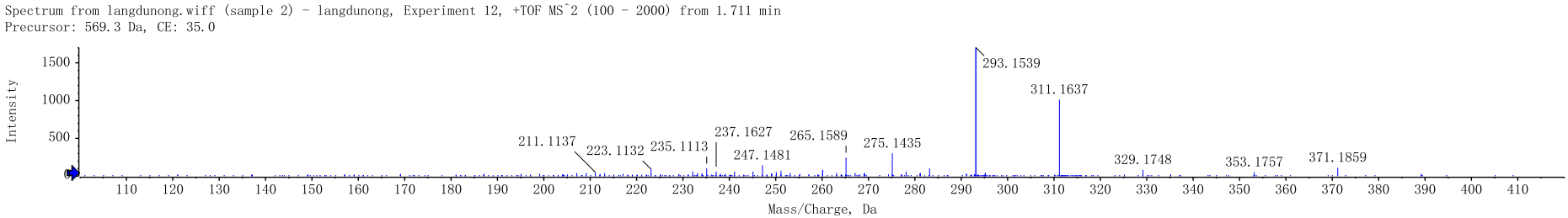

Figure S17. MSMS spectrogram of peak 3

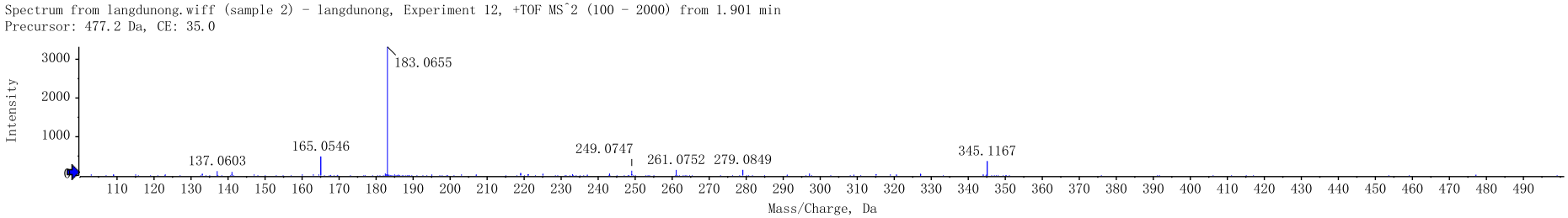

Figure S18. MSMS spectrogram of peak 4

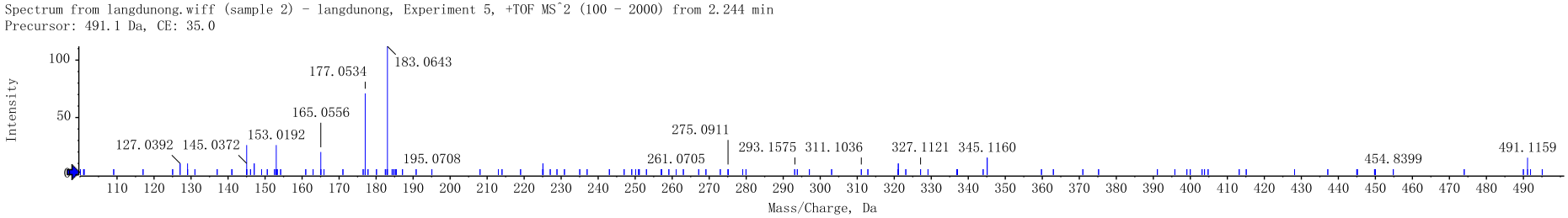

Figure S19. MSMS spectrogram of peak 5

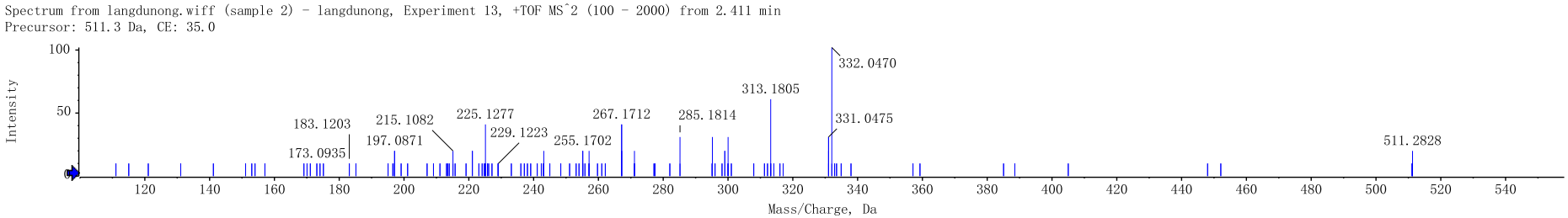

Figure S20. MSMS spectrogram of peak 6

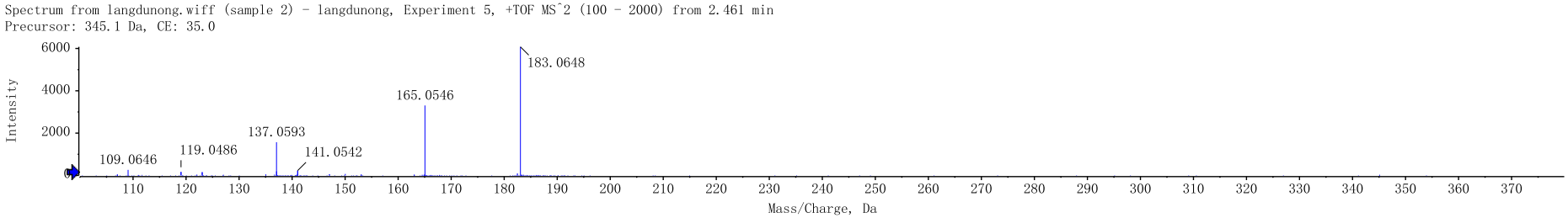

Figure S21. MSMS spectrogram of peak 7

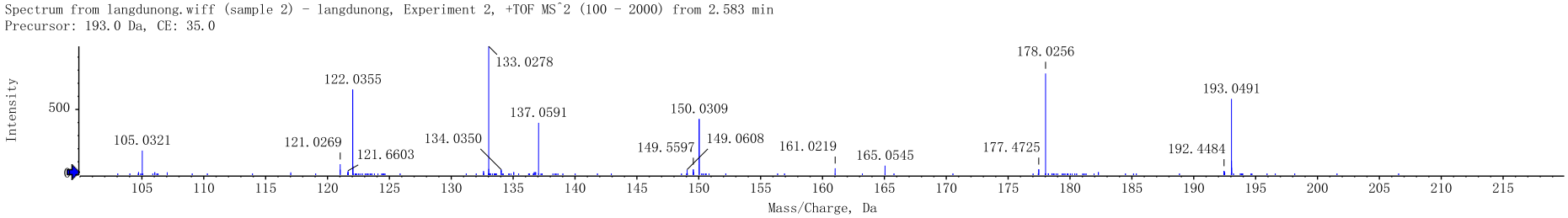

Figure S22. MSMS spectrogram of peak 8

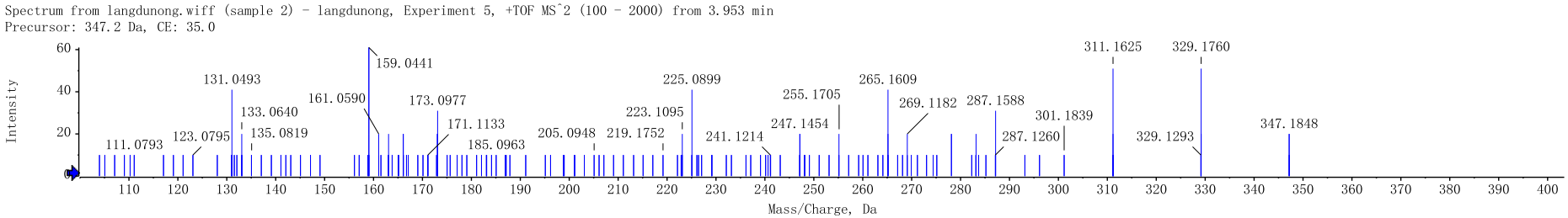

Figure S23. MSMS spectrogram of peak 9

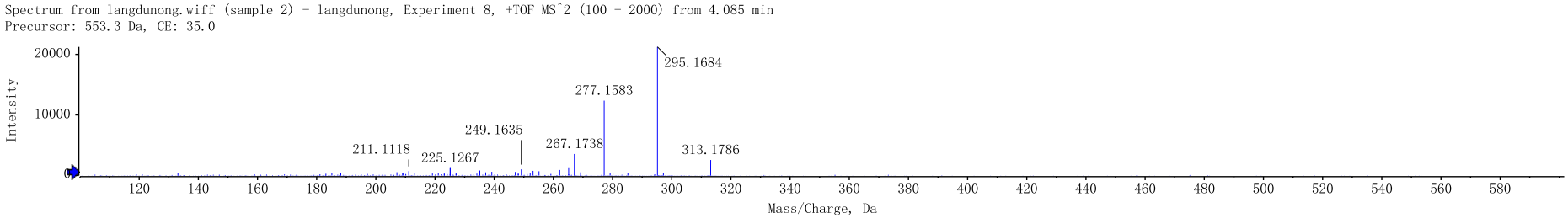

Figure S24. MSMS spectrogram of peak 10

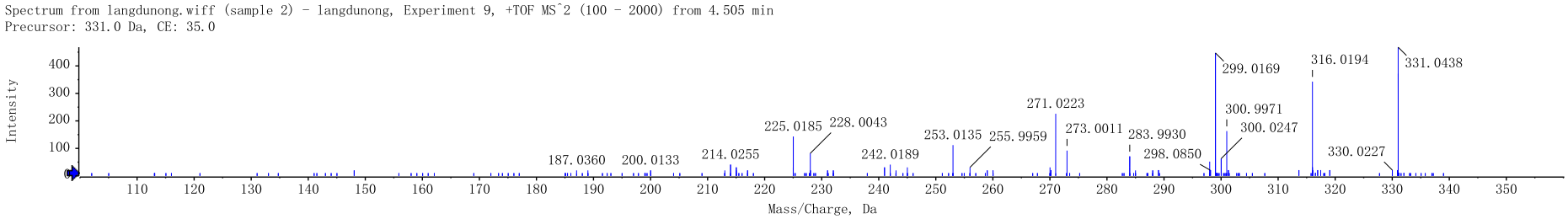

Figure S25. MSMS spectrogram of peak 11

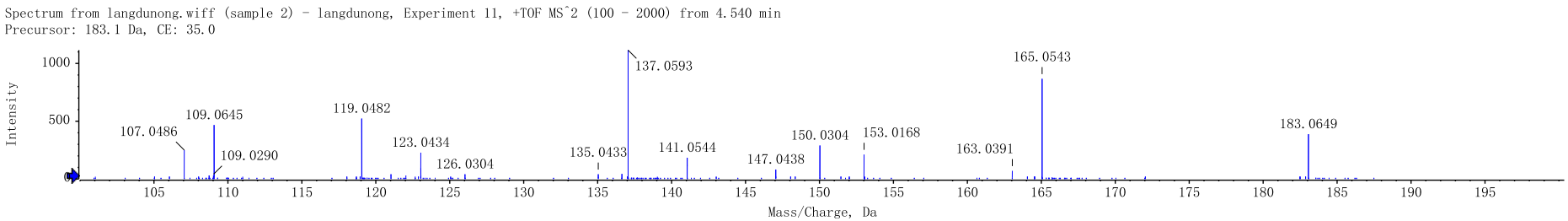

Figure S26. MSMS spectrogram of peak 12

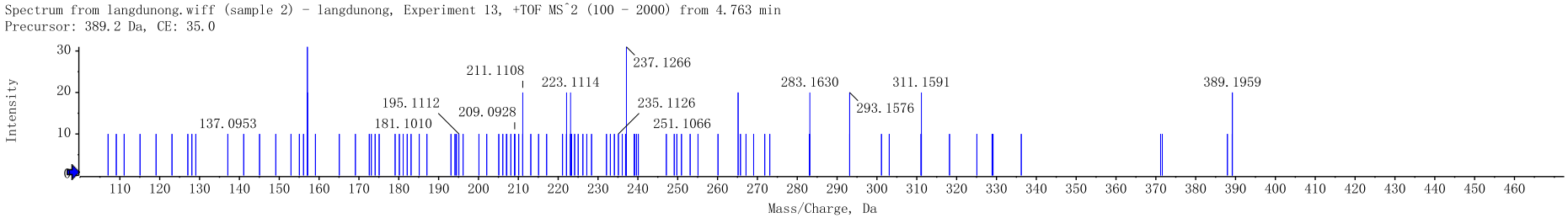

Figure S27. MSMS spectrogram of peak 13

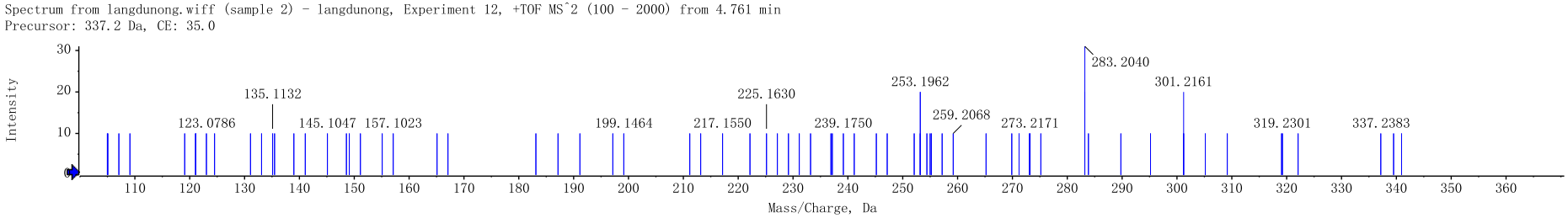

Figure S28. MSMS spectrogram of peak 14

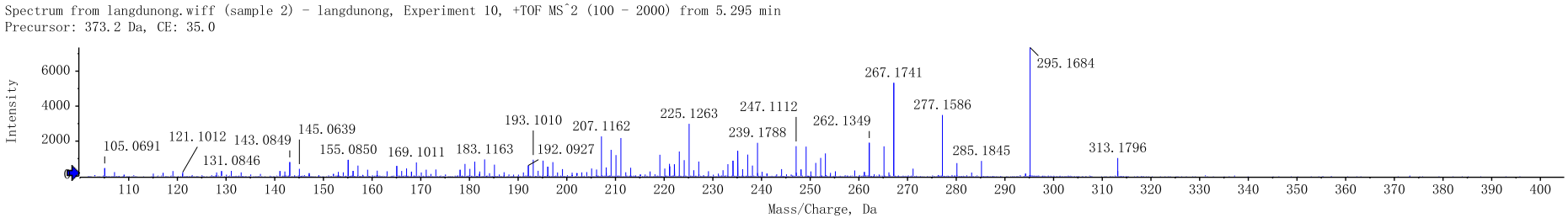

Figure S29. MSMS spectrogram of peak 15

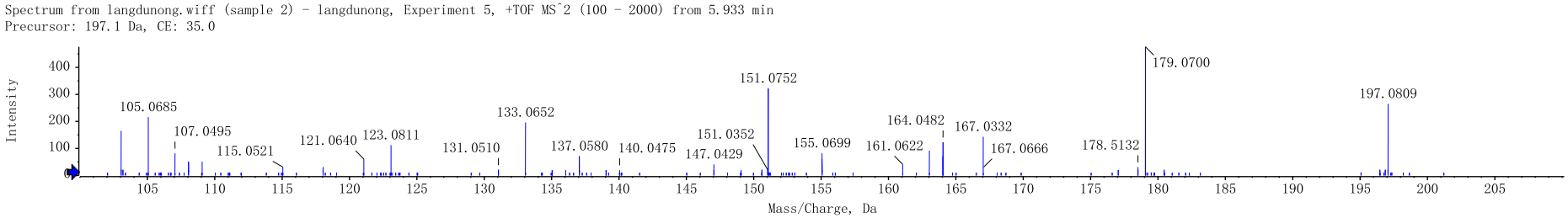

Figure S30. MSMS spectrogram of peak 16

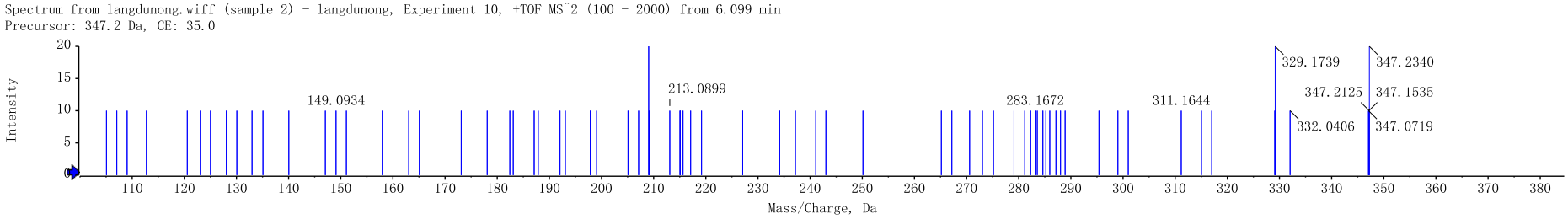

Figure S31. MSMS spectrogram of peak 17

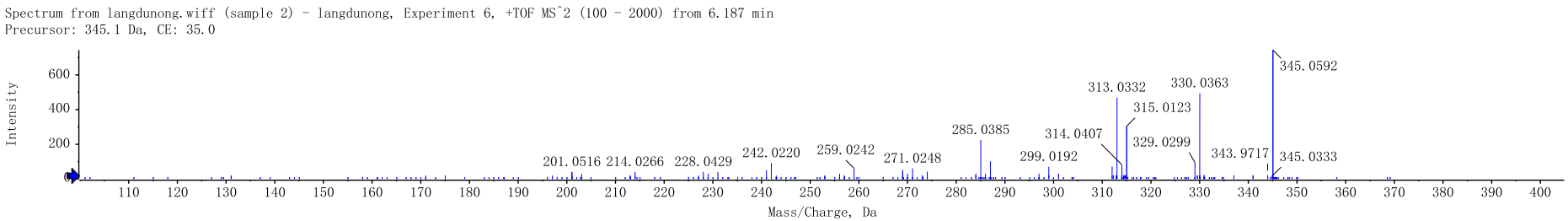

Figure S32. MSMS spectrogram of peak 18

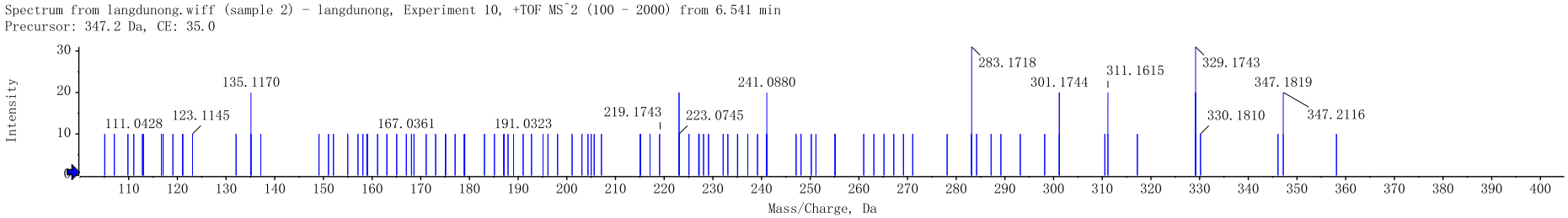

Figure S33. MSMS spectrogram of peak 19

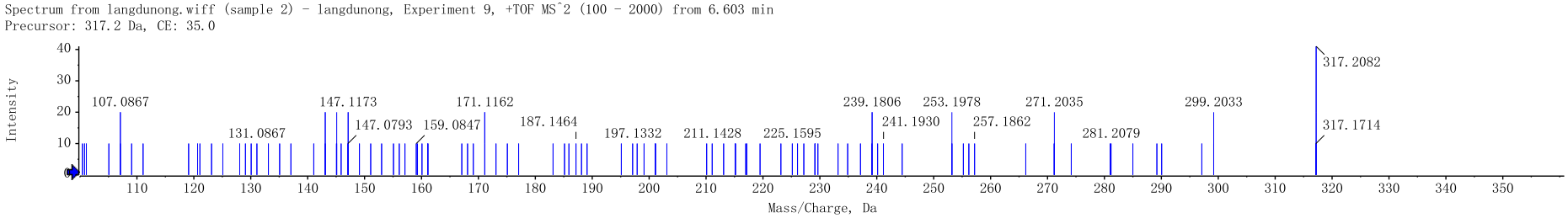

Figure S34. MSMS spectrogram of peak 20

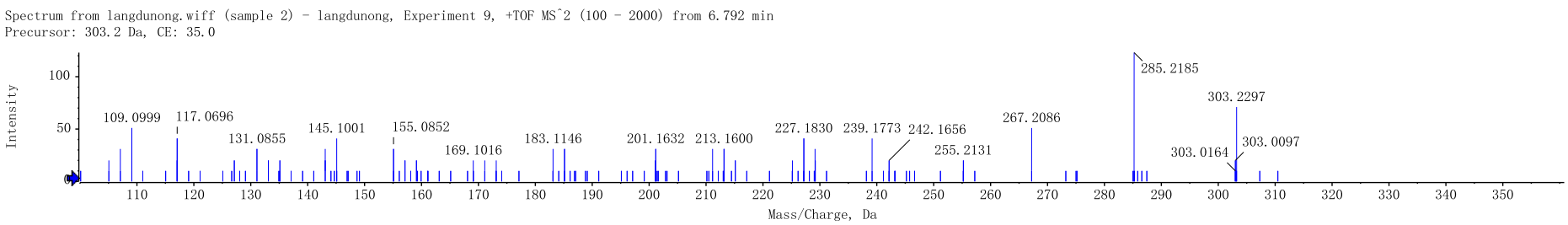

Figure S35. MSMS spectrogram of peak 21

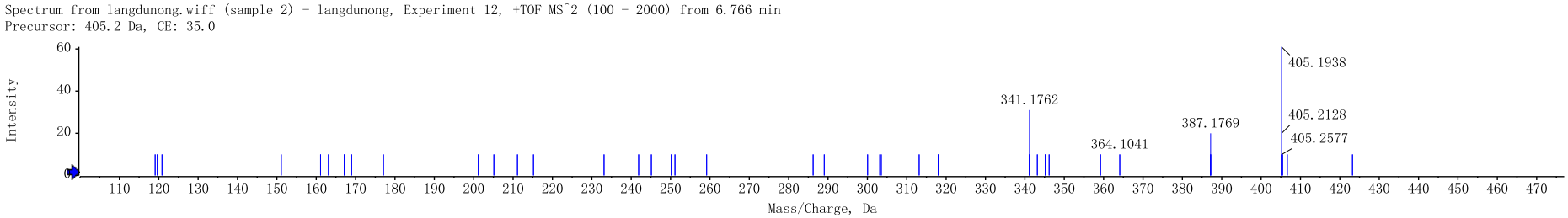

Figure S36. MSMS spectrogram of peak 22

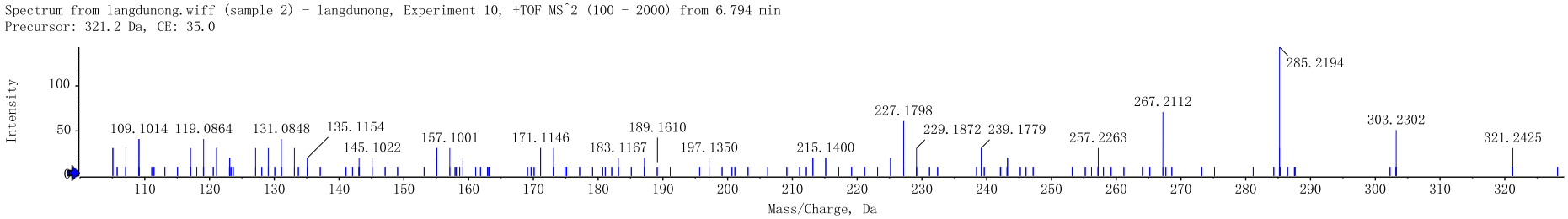

Figure S37. MSMS spectrogram of peak 23

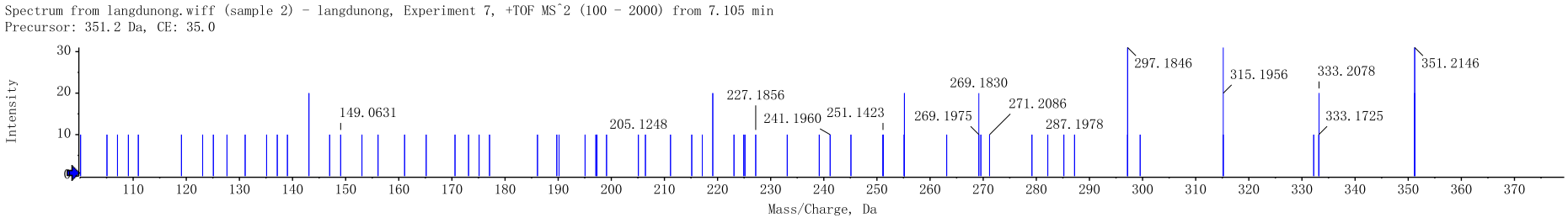

Figure S38. MSMS spectrogram of peak 24

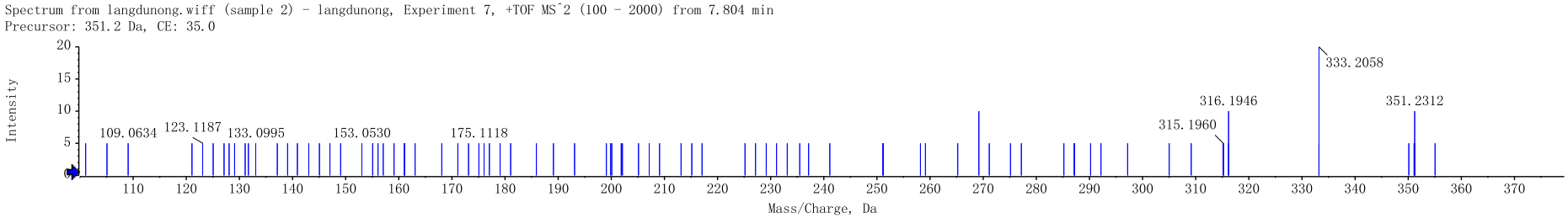

Figure S39. MSMS spectrogram of peak 25

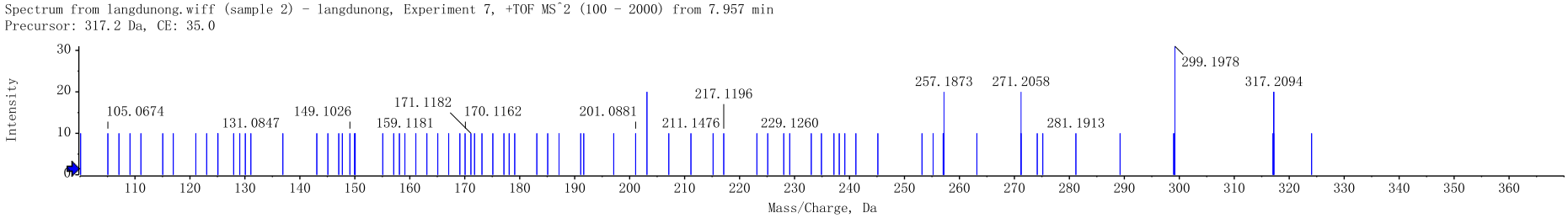

Figure S40. MSMS spectrogram of peak 26

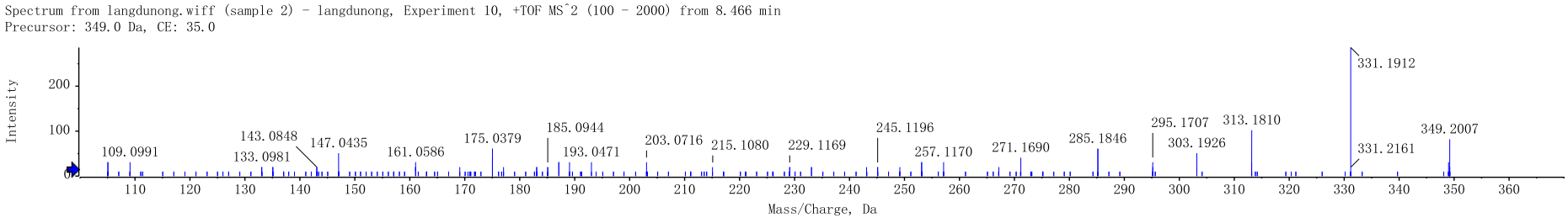

Figure S41. MSMS spectrogram of peak 27

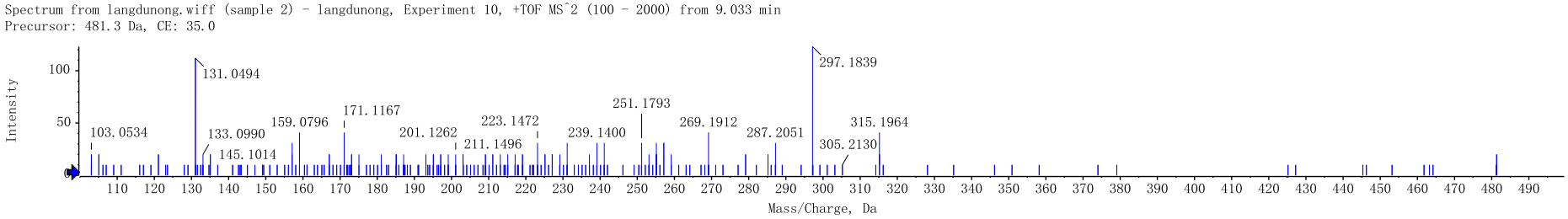

Figure S42. MSMS spectrogram of peak 28

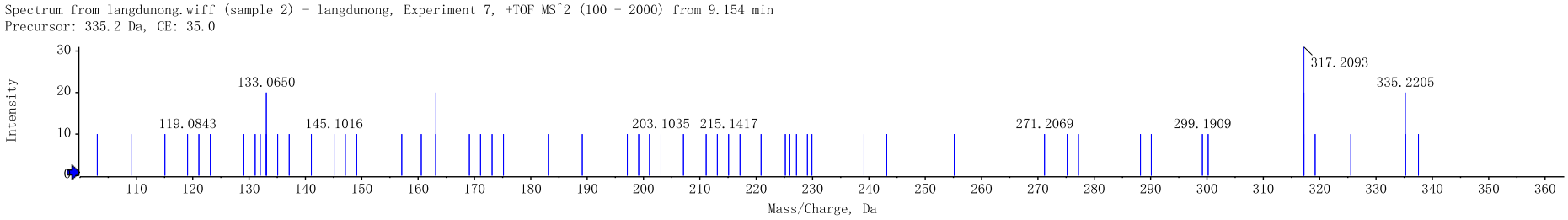

Figure S43. MSMS spectrogram of peak 29

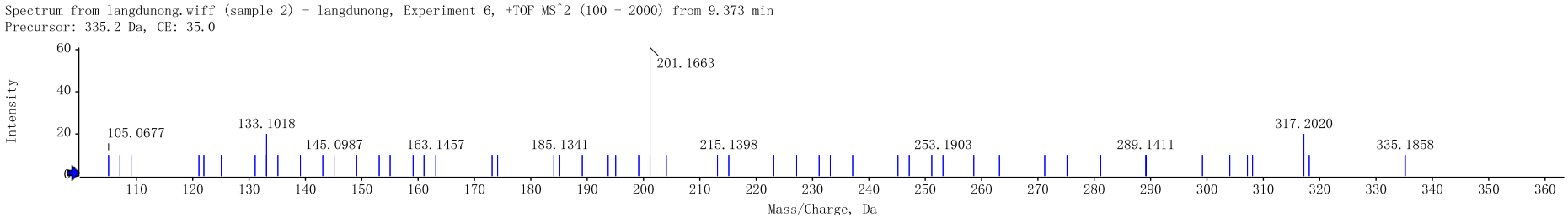

Figure S44. MSMS spectrogram of peak 30

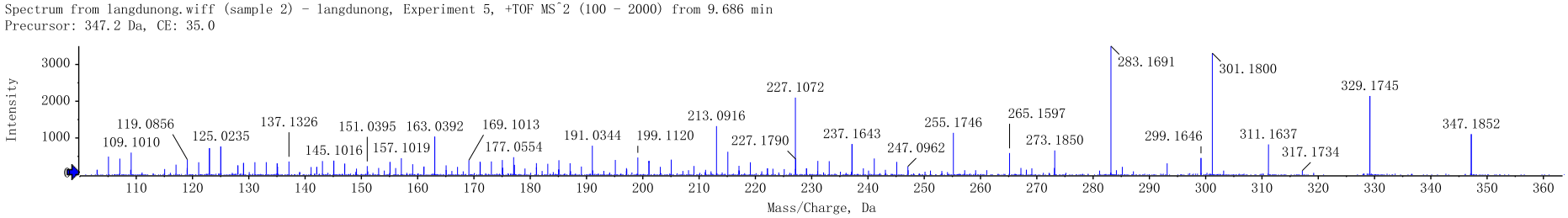

Figure S45. MSMS spectrogram of peak 31

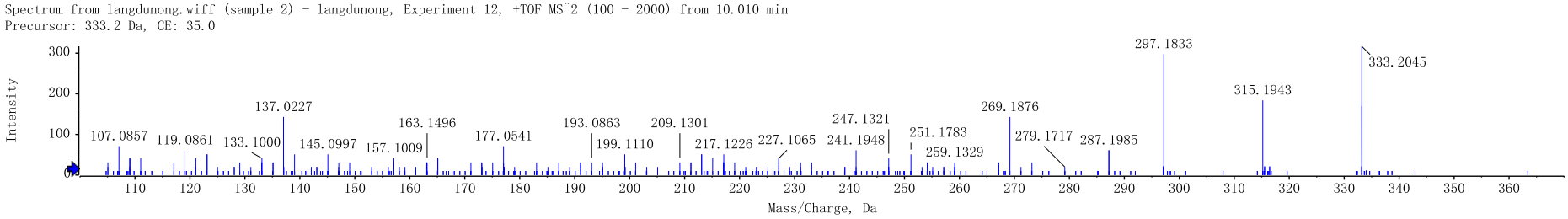

Figure S46. MSMS spectrogram of peak 32

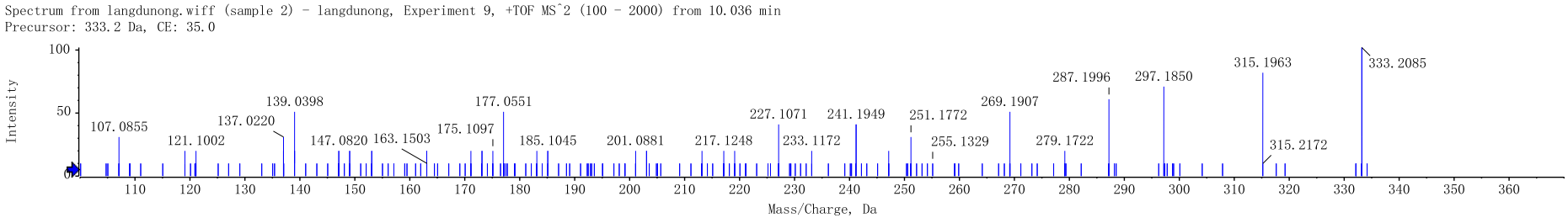

Figure S47. MSMS spectrogram of peak 33

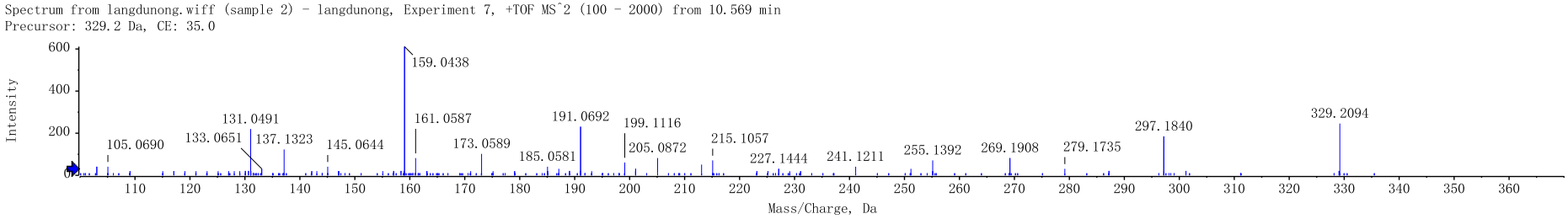

Figure S48. MSMS spectrogram of peak 34

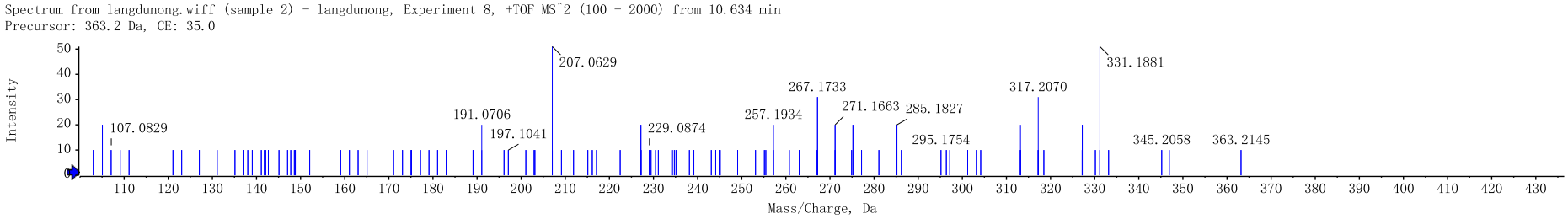

Figure S49. MSMS spectrogram of peak 35

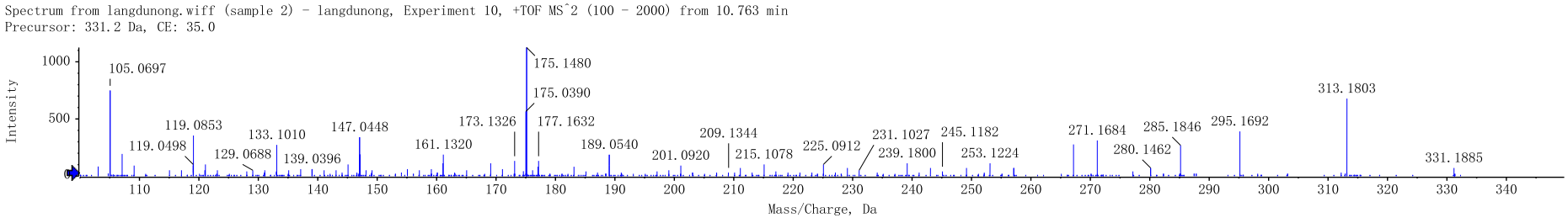

Figure S50. MSMS spectrogram of peak 36

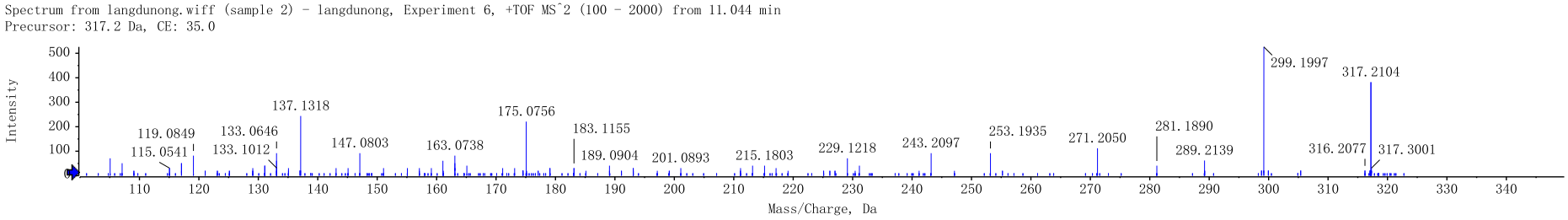

Figure S51. MSMS spectrogram of peak 37

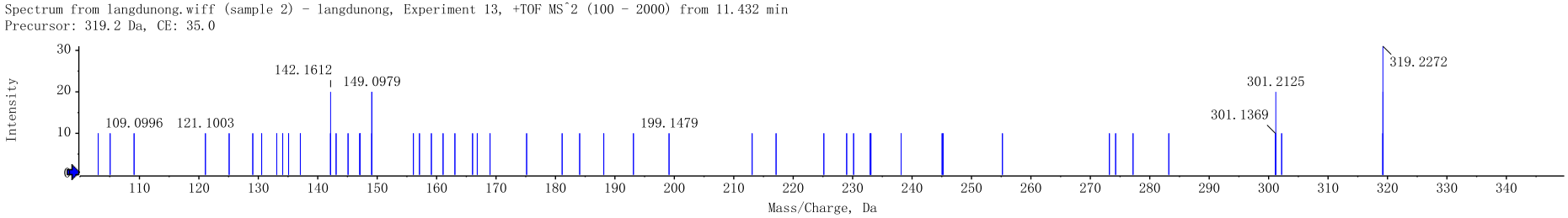

Figure S52. MSMS spectrogram of peak 38

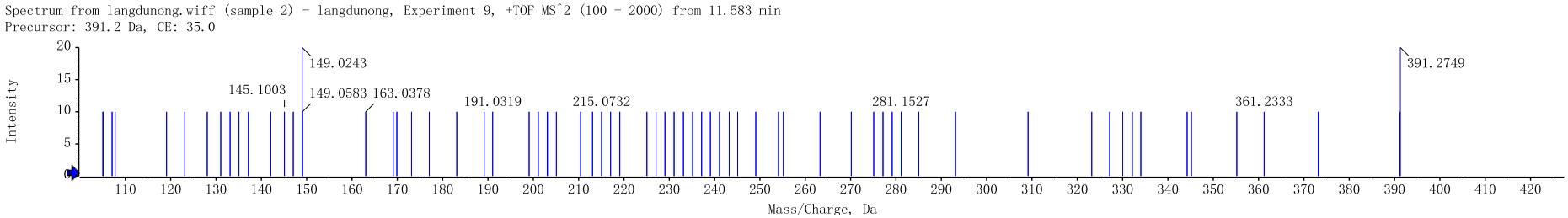

Figure S53. MSMS spectrogram of peak 39

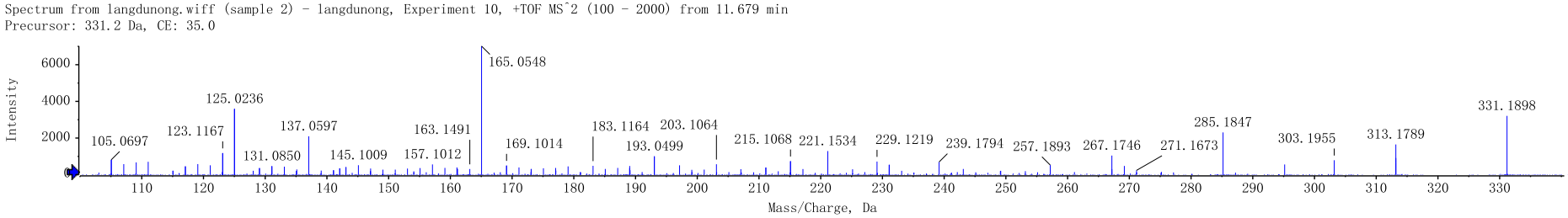

Figure S54. MSMS spectrogram of peak 40

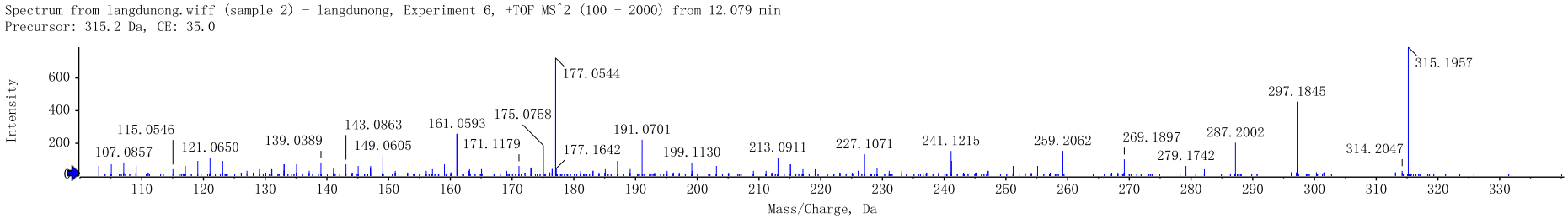

Figure S55. MSMS spectrogram of peak 41

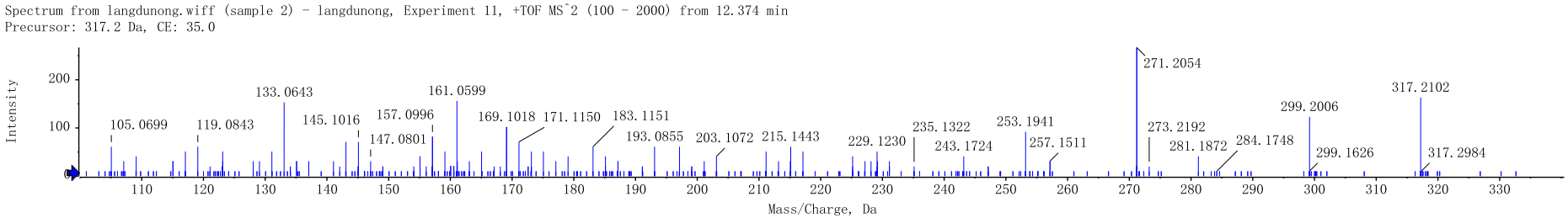

Figure S56. MSMS spectrogram of peak 42

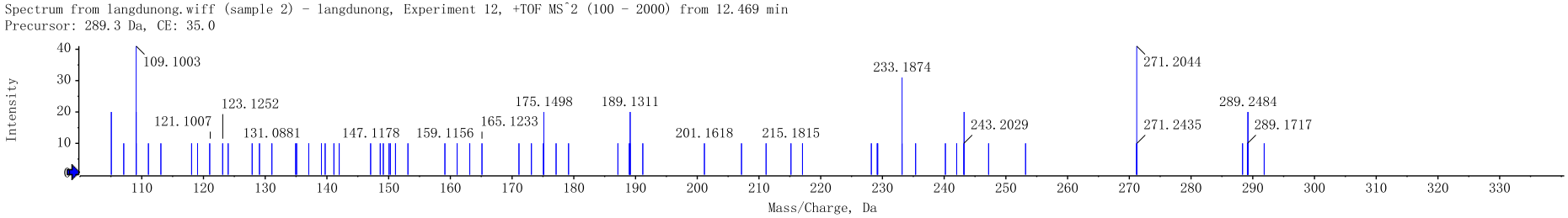

Figure S57. MSMS spectrogram of peak 43

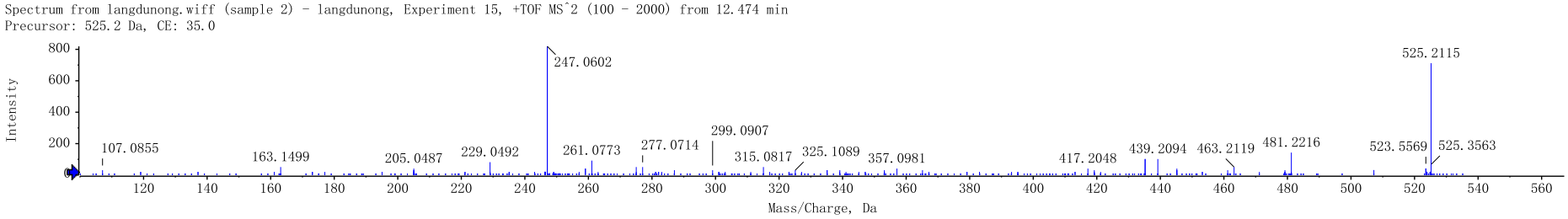

Figure S58. MSMS spectrogram of peak 44

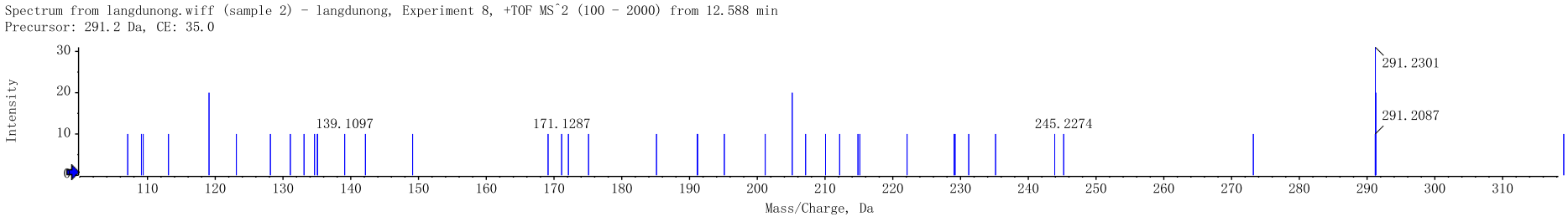

Figure S59. MSMS spectrogram of peak 45

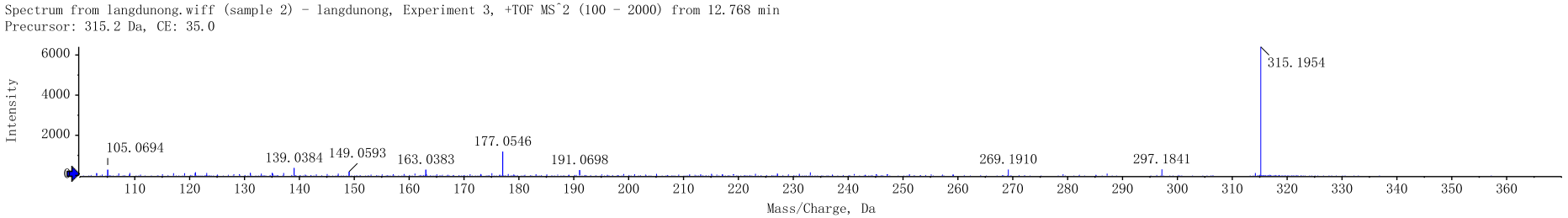

Figure S60. MSMS spectrogram of peak 46

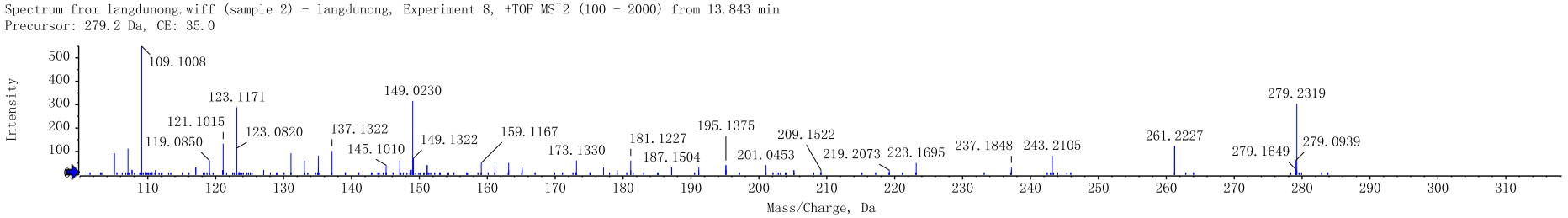

Figure S61. MSMS spectrogram of peak 47

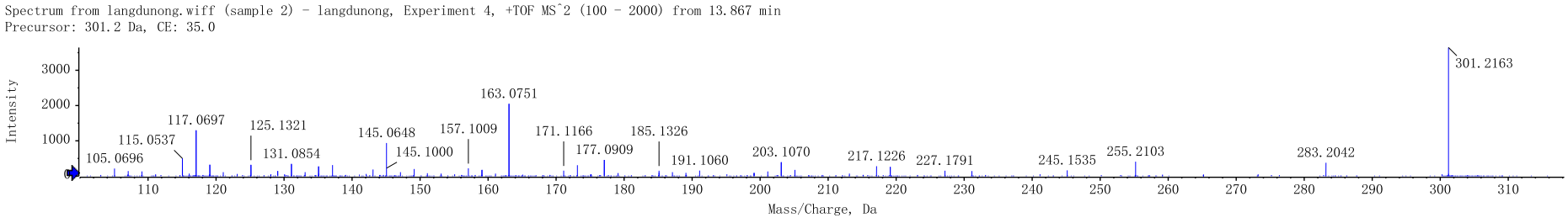

Figure S62. MSMS spectrogram of peak 48

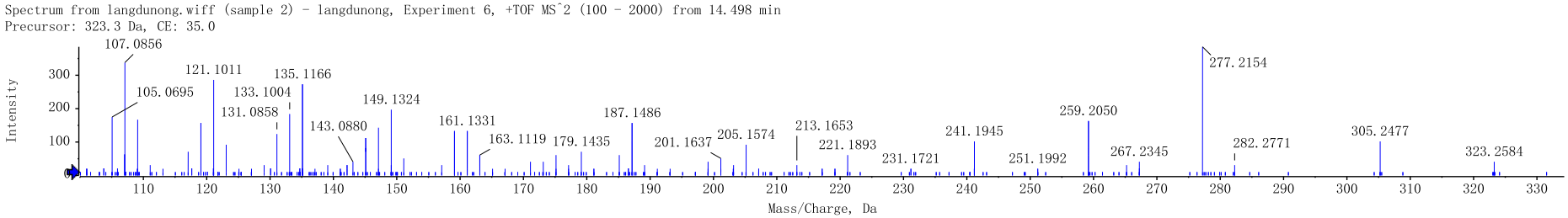

Figure S63. MSMS spectrogram of peak 49

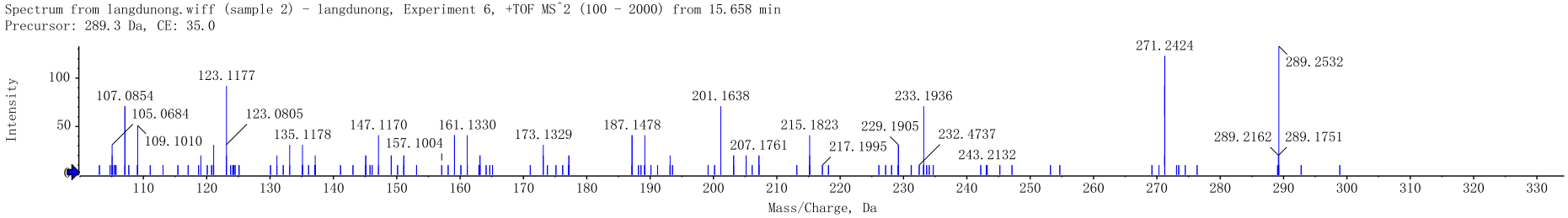

Figure S64. MSMS spectrogram of peak 50

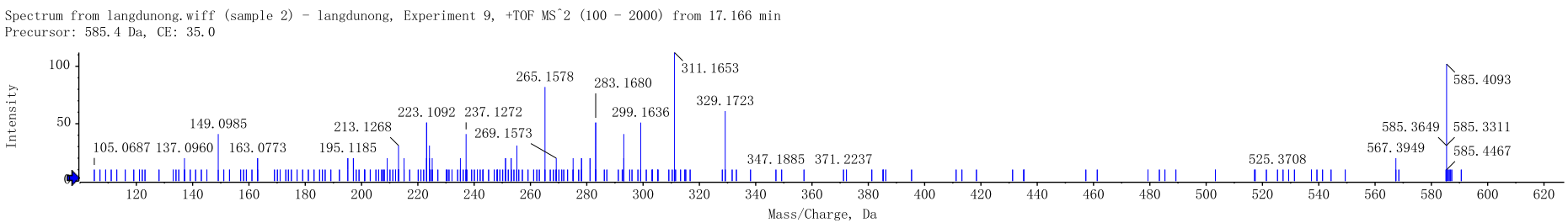

Figure S65. MSMS spectrogram of peak 51

Tables

Table S1. Regression data, LODs and LOQs for four compounds

Analyte	Calibratio curve	r^2	Linearity range (μg/mL)	LOD (ng/mL)	LOQ (ng/mL)
jolkinolide A	y = 0.1132x + 0.0223	0.9993	0.97-4.35	1.71	5.64
jolkinolide B	y = 0.0538x + 0.2097	0.9961	5.71-25.70	0.92	2.99
17-hydroxyjolkinolide A	y = 0.0281x + 0.0824	0.9911	5.01-22.54	4.12	13.60
17-hydroxyjolkinolide B	y = 0.0153x + 0.1993	0.9956	18.46-83.09	13.15	43.44

Table S2. Precision and recovery of four active components (n = 3)

Analyte	Intraday RSD		Interday RSD		Amount added (mg)	Recovery (%)	RSD (%)
	Rt (%)	Pa (%)	Rt (%)	Pa (%)			
jolkinolide A	0.10	4.65	0.13	4.13	0.22	97.8	2.68
					0.44	92.3	
					0.65	94.6	
jolkinolide B	0.12	2.81	0.15	3.15	1.21	98.0	3.74
					2.42	102.3	
					3.63	106.3	
17-hydroxyjolkinolide A	0.19	3.35	0.21	3.89	0.53	93.0	4.98
					1.06	98.9	
					1.58	104.2	
17-hydroxyjolkinolide B	0.34	3.24	0.29	3.54	3.52	95.9	4.44
					7.03	105.2	
					10.55	97.8	

Table S3. Experimental design applied to extraction and responses of α-glucosidase inhibition activities and contents of steroid saponins in Box-Behnken design (BBD) assays

Run	Independent variables			Responses			
	ethanol concentration	extraction temperature	time	Y_1	Y_2	Y_3	Y_4
	%	℃	h	mg/g	mg/g	mg/g	mg/g

1	75	60	1.5	0.1557	0.8573	0.3937	2.4628
2	75	60	1.5	0.1522	0.8491	0.3985	2.3761
3	100	40	1.5	0.1504	0.8956	0.4016	2.1944
4	50	40	1.5	0.1246	0.6657	0.2957	1.8910
5	75	60	1.5	0.1540	0.8361	0.3880	2.2262
6	75	40	1.5	0.1433	0.7825	0.3220	1.9803
7	50	60	2.0	0.1484	0.7130	0.3611	2.0081
8	75	40	2.0	0.1416	0.7924	0.3282	1.9605
9	100	60	1.0	0.1397	0.8420	0.3684	2.4287
10	75	80	2.0	0.2014	0.7961	0.3662	2.0725
11	50	80	1.5	0.1750	0.7029	0.3846	1.5952
12	50	60	1.0	0.1469	0.8899	0.3904	2.4064
13	75	60	1.5	0.1465	0.8598	0.3892	2.3138
14	100	60	2.0	0.1639	0.9645	0.4327	2.8132
15	75	60	1.5	0.1577	0.8991	0.4099	2.4843
16	75	80	1.0	0.1744	0.8130	0.3662	2.3769
17	100	80	1.5	0.1508	0.9021	0.4035	2.5937

Table S4. ANOVA statistics of the quadratic model for the extraction yields of jolkinolide A, jolkinolide B, 17-hydroxyjolkinolide A and 17-hydroxyjolkinolide B

Source	Y_1		Y_2		Y_3		Y_4	
	F Value	P-Value Prob>F	F Value	P-Value Prob>F	F Value	P-Value Prob>F	F Value	P-Value Prob>F
Model	12.29	0.0016	7.98	0.0061	12.44	0.0016	9.73	0.0033
X_1	0.30	0.5998	39.45	0.0004	23.46	0.0019	37.35	0.0005
X_2	62.64	<0.0001	0.60	0.4643	23.05	0.0020	3.09	0.1224

X_3	8.10	0.0248	0.37	0.5612	1.30	0.2915	0.94	0.3642
X_1X_2	15.61	0.0055	0.19	0.6797	11.66	0.0112	7.96	0.0257
X_1X_3	3.19	0.1172	17.67	0.0040	13.47	0.0080	10.10	0.0155
X_2X_3	5.12	0.0581	0.14	0.7183	0.06	0.8120	1.33	0.2861
X_1^2	8.94	0.0202	0.13	0.7332	2.10	0.1907	0.01	0.9203
X_2^2	4.07	0.0833	12.98	0.0087	29.11	0.0010	26.72	0.0013
X_3^2	3.44	0.1061	0.01	0.9214	7.25	0.0310	0.34	0.5760
Lack of fit	3.84	0.1131	3.98	0.1079	3.48	0.1298	1.78	0.2902

Table S5. Compounds identified in *E. fischeriana* by UPLC-Q-TOF-MS/MS in positive ion mode

No.	T_R (min)	$[M+H]^+$	Error (ppm)	Formula	Fragment ions in positive ion mode	Identification
1	1.19	637.1000	-3.6	$C_{27}H_{24}O_{18}$	619, 449, 279, 109	1,3,6-tri-O-galloyl-β-D-allopyranose
2	1.44	637.1022	-1.3	$C_{27}H_{24}O_{18}$	619, 449, 279, 109	1,2,6-tri-O-galloyl-β-D-allopyranose
3	1.73	569.2590	-0.3	$C_{28}H_{40}O_{12}$	389, 371, 353, 329, 311, 293, 275, 265	fischeroside C
4	1.88	477.1603	0.1	$C_{20}H_{28}O_{13}$	345, 185, 166	2,4-dihydroxy-6-methoxyacetophenoe-4-O-α-L-arabinofuranosyl(1→6)-β-D-glucopyranoside
5	2.23	491.1743	-3.3	$C_{21}H_{30}O_{13}$	345, 183, 177, 165, 153, 145	2,4-dihydroxy-6-methoxyacetophenoe-5-methyl-4-O-α-L-rhamnosyl(1→6)-β-D-glucopyranoside
6	2.40	511.2527	-2.1	$C_{26}H_{38}O_{10}$	331, 313, 295, 285, 267, 257	euphopiloside A
7	2.45	345.1176	-1.2	$C_{15}H_{20}O_9$	183, 165, 137	2,4-dihydroxy-6-methoxyacetophenoe 4-O-β-D-glucopyranoside
8	2.61	193.0495	-0.2	$C_{10}H_8O_4$	178, 165, 161, 150, 137, 133, 122, 105	scopoletin
9	3.95	347.1846	-1.7	$C_{20}H_{26}O_5$	329, 311, 265, 287, 173, 159	11α,17-dihydroxyhelioscopinolide E
10	4.09	553.2637	-1.2	$C_{28}H_{40}O_{11}$	313, 295, 277, 267, 255	fischeroside A
11	4.52	331.0444	-1.3	$C_{16}H_{10}O_8$	316, 299, 271, 253, 225	3,8-dihydroxy-2,7-dimethoxychromeno[5,4,3-cde]chromene-5,10-dione
12	4.57	183.0653	0.6	$C_9H_{10}O_4$	165, 153, 150, 141, 137, 123, 119, 109	1-(2,4-dihydroxy-6-methoxyphenyl)ethanone

13	4.74	389.1959	-3.8	$C_{22}H_{28}O_6$	311, 293, 283, 237	17-acetoxyjolkinolide B
14	4.76	337.2368	-1.6	$C_{20}H_{32}O_4$	319, 301, 283, 253, 225	3S,16S,17-trihydroxy-2-one-ent-kaurane
15	5.30	373.2010	0.1	$C_{22}H_{28}O_5$	313, 295, 277, 267, 255	17-acetoxyjolkinolide A
16	5.92	197.0808	1.8	$C_{10}H_{12}O_4$	179, 167, 164, 151, 133, 123, 107, 105	3-acetyl-2,6-dihydroxy-4-methoxybenzaldehyde
17	6.10	347.1852	-0.3	$C_{20}H_{26}O_5$	329, 311, 283, 215, 213, 149	(3aR,6aS,10R,10aR,10bS)-3a,10a-dihydroxy-5-(hydroxymethyl)-2,10-dimethyl-7-(propan-2-ylidene)-3a,4,6a,7,10,10a-hexahydrobenzo[e]azulene-3,8(9H,10bH)-dione.
18	6.18	345.0608	-0.8	$C_{17}H_{12}O_8$	330, 315, 313, 287, 242	3-hydroxy-2,7,8-trimethoxychromeno[5,4,3-cde]chromene-5,10-dione
19	6.54	347.1847	-1.7	$C_{20}H_{26}O$	329, 283, 311, 301, 241	(3aR,6aS,7R,10R,10aR,10bS)-3a,10a-dihydroxy-5-(hydroxymethyl)-2,10-dimethyl-7-(prop-1-en-2-yl)-3a,4,6a,7,10,10a-hexahydrobenzo[e]azulene-3,8(9H,10bH)-dione
20	6.59	317.2105	-2.0	$C_{20}H_{28}O_3$	299, 271, 253, 239, 171, 147	atis-16-en-13(S)-hydroxy-3,14-dione
21	6.75	303.2297	-1.5	$C_{20}H_{30}O_2$	285, 267, 257, 227, 215, 213, 211, 185, 183	ent-(3α,5β,8α,9β,10α, 12α)-3-hydroxyatis-16-en-14-one
22	6.75	405.1941	8.2	$C_{22}H_{28}O_7$	387, 341	20-oxo-prostratin
23	6.78	321.2422	0.2	$C_{20}H_{32}O_3$	303, 285, 267, 239, 227, 171, 157, 131, 119	ent-(16R)-16,17-dihydroxykauran-3-one
24	7.11	351.2163	-0.9	$C_{20}H_{30}O_5$	333, 315, 297, 287, 269	yuexiandajisu E
25	7.80	351.2153	-3.7	$C_{20}H_{30}O_5$	333, 316, 269	yuexiandajisu D
26	7.95	317.2103	-2.6	$C_{20}H_{28}O_3$	299, 281, 271, 257	ent-3β-hydroxyatis-16-ene-2,14-dione
27	8.45	349.2002	-2.2	$C_{20}H_{28}O_5$	331, 313, 295, 285, 267, 175, 147	7β,11β,12β-trihydroxy-ent-abieta-8(14),13(15)-dien-16,12-olide
28	9.01	481.2590	1.1	$C_{29}H_{36}O_6$	315, 297, 287, 269	jolkinol A
29	9.14	335.2211	-1.8	$C_{20}H_{30}O_4$	317, 299, 271, 215, 203, 145, 133, 119	alboatisin A
30	9.36	335.2210	-2.1	$C_{20}H_{30}O_4$	317, 289, 253, 201	8β,14α-dihydroxyabiet-13(15)-ene-16,12-lactone
31	9.68	347.1844	-2.6	$C_{20}H_{26}O_5$	329, 311, 301, 283, 273, 265, 255, 237,	17-hydroxyjolkinolide B

					227, 213, 191, 163	
32	9.99	333.2063	0.9	$C_{20}H_{28}O_4$	315, 297, 269, 241, 217, 199, 177, 137, 119	fischeriolide A
33	10.17	333.2057	-1.0	$C_{20}H_{28}O_4$	315, 297, 287, 269, 251, 241, 227, 177, 139	fischeriolide C
34	10.56	329.2116	1.3	$C_{21}H_{28}O_3$	297, 269, 255, 241, 215, 205, 191, 173, 161, 159, 137, 131	(Z)-methyl 2-((4bR,8aR)-4b,8,8-trimethyl-3-oxo-4b,5,6,7,8,8a,9,10-octahydrophenanthren-2(3H)-ylidene)propanoate
35	10.59	363.2161	-1.4	$C_{21}H_{30}O_5$	345, 311, 317, 295, 285, 267, 257, 175	euphorin H
36	10.75	331.1902	-0.6	$C_{20}H_{26}O_4$	313, 295, 285, 271, 267, 175	17-hydroxyjolkinolide A
37	11.00	317.2111	-0.1	$C_{20}H_{28}O_3$	299, 289, 281, 271, 253, 175	ent-11β-hydroxyabieta-8(14),13(15)-dien-16,12β-olide
38	11.41	319.2242	-8.1	$C_{20}H_{30}O_3$	301, 199	ent-3β,(13S)-dihydroxyatis-16-en-14-one
39	11.58	391.2117	0.5	$C_{22}H_{30}O_6$	281, 215	prostratin
40	11.67	331.1895	-2.7	$C_{20}H_{26}O_4$	313, 285, 267, 221, 193, 165, 137, 125	jolkinolide B
41	12.10	315.1952	-0.9	$C_{20}H_{26}O_3$	297, 287, 269, 227, 177, 175, 161, 149	jolkinolide A
42	12.36	317.2107	-1.3	$C_{20}H_{28}O_3$	317, 299, 271, 253, 169, 161, 157, 133	euphopilolide
43	12.40	289.2145	-5.9	$C_{19}H_{28}O_2$	271, 233, 109	fischeria A
44	12.47	525.2115	-0.6	$C_{29}H_{32}O_9$	481, 463, 445, 439, 275	langduin D
45	12.58	291.2324	1.9	$C_{19}H_{30}O_2$	245, 171, 139	ent-kaurane-3-oxo-16α,17-diol
46	12.73	315.1956	0.3	$C_{20}H_{26}O_3$	297, 269, 191, 177, 163, 149, 139, 105	(1aR,7aR,11aR,11cR)-4,8,8,11a-tetramethyl-6,7,7a,8,9,10,11,11a,11b,11c-decahydro-3H-oxireno[2',3':3,4]phenanthro[3,2-b]furan-3-one
47	13.82	279.2316	-0.9	$C_{18}H_{30}O_2$	261, 243, 149, 123, 109	α-linolenic acid
48	13.85	301.2161	-0.4	$C_{20}H_{28}O_2$	283, 255, 173, 145	ent-atis-16(17)-ene-3,14-dione
49	14.49	323.2580	-1.5	$C_{20}H_{34}O_3$	305, 277, 259, 241, 205, 187, 149	ent-atisane-3β,16α,17-triol
50	15.63	289.2521	-1.7	$C_{20}H_{32}O$	271, 233, 201	ent-kaur-16-en-14-ol
51	17.15	585.4152	0.4	$C_{36}H_{56}O_6$	329, 311, 299, 265, 237, 223, 213	12-deoxyphorbaldehyde-13-hexadecanoate